

like receptor; STAT = signal transducer and activator of transcription; IRF = interferon regulatory factor; ISRE = interferon-stimulated response element; IRE = interferon regulatory factor-recognition element; HSPs = heat shock proteins; CSF = cerebrospinal fluid; GPCR = G protein-coupled receptor; RGS = regulator of G protein signaling.

Competing interests

The author(s) declare that they have no competing interests.

Authors' contributions

JS, YN and HT carried out DNA microarray and real-time RT-PCR analysis, and JS drafted the manuscript. TY participated in the design of the study and helped to draft the manuscript. All authors read and approved the final manuscript.

Additional material

Additional File 1

The gene list of cDNA microarray utilized in the present study. The complete gene list of cDNA microarray utilized in the present study is shown. It includes 1,258 well-annotated genes, selected from cytokines, growth factors and their receptors, apoptosis regulators, oncogenes, transcription factors, cell cycle regulators and housekeeping genes.

Click here for file

[<http://www.biomedcentral.com/content/supplementary/1471-2377-6-18-S1.xls>]

Additional File 2

Scatter plots of three distinct microarray experiments. The figure represents a scatter plot exhibiting the comparison between the fluorescence intensity (FI) of C γ 5 signals in the longitudinal axis and FI of C γ 3 signals in the horizontal axis. (a) the subject #1 (a 46 year-old healthy man), (b) the subject #2 (a 28 year-old healthy man), and (c) the subject #4 (a 27 year-old woman with RRMS who was a dropout of IFN β treatment due to induction of frequent severe relapses).

Click here for file

[<http://www.biomedcentral.com/content/supplementary/1471-2377-6-18-S2.ppt>]

Additional File 3

The complete list of upregulated genes in PBMC following exposure to IFN β for 3 hours. Upregulated genes in PBMC of the subject #1 (a 46 year-old healthy man) by a 3 hour-exposure to 50 ng/ml recombinant human IFN β are listed with C γ 5/C γ 3 signal intensity ratio, gene symbol, GenBank accession number, and gene name. *In vivo* IRG in T cells and non-T cells of RRMS patients reported previously (Ref. 16) are underlined.

Click here for file

[<http://www.biomedcentral.com/content/supplementary/1471-2377-6-18-S3.xls>]

Additional File 4

The complete list of downregulated genes in PBMC following exposure to IFN β for 3 hours. Downregulated genes in PBMC of the subject #1 (a 46 year-old healthy man) by a 3 hour-exposure to 50 ng/ml recombinant human IFN β are listed with C γ 5/C γ 3 signal intensity ratio, gene symbol, GenBank accession number, and gene name.

Click here for file

[<http://www.biomedcentral.com/content/supplementary/1471-2377-6-18-S1.xls>]

Additional File 5

The complete list of upregulated genes in PBMC following exposure to IFN β for 24 hours. Upregulated genes in PBMC of the subject #1 (a 46 year-old healthy man) by a 24 hour-exposure to 50 ng/ml recombinant human IFN β are listed with C γ 5/C γ 3 signal intensity ratio, gene symbol, GenBank accession number, and gene name. *In vivo* IRG in T cells and non-T cells of RRMS patients reported previously (Ref. 16) are underlined.

Click here for file

[<http://www.biomedcentral.com/content/supplementary/1471-2377-6-18-S5.xls>]

Additional File 6

The complete list of downregulated genes in PBMC following exposure to IFN β for 24 hours. Downregulated genes in PBMC of the subject #1 (a 46 year-old healthy man) by a 24 hour-exposure to 50 ng/ml recombinant human IFN β are listed with C γ 5/C γ 3 signal intensity ratio, gene symbol, GenBank accession number, and gene name.

Click here for file

[<http://www.biomedcentral.com/content/supplementary/1471-2377-6-18-S6.xls>]

Additional File 7

Top 20 upregulated genes in PBMC following exposure to IFN β for 3 hours: two additional subjects. Upregulated genes in PBMC of the subject #2 (a 28 year-old healthy man) and #4 (a 27 year-old woman with RRMS who was a dropout of IFN β treatment due to induction of frequent severe relapses) following a 3 hour-exposure to 50 ng/ml recombinant human IFN β are listed with C γ 5/C γ 3 signal intensity ratio, gene symbol, and gene name. Both CXCR3 ligand (yellow) and CCR2 ligand (blue) chemokines are highlighted.

Click here for file

[<http://www.biomedcentral.com/content/supplementary/1471-2377-6-18-S7.xls>]

Acknowledgements

This work was supported by grants to J-IS from Research on Psychiatric and Neurological Diseases and Mental Health, the Ministry of Health, Labour and Welfare of Japan (H17-020) and Research on Health Sciences Focusing on Drug Innovation, the Japan Health Sciences Foundation (KH21101), and by the Grant-in-Aid for Scientific Research, the Ministry of Education, Culture, Sports, Science and Technology of Japan (B-18300118). The authors would thank Dr. Jun Tsuyuzaki, Department of Neurology, Komoro Kosei Hospital, Nagano, Japan for introducing us the patients.

References

1. Sospedra M, Martin R: Immunology of multiple sclerosis. *Annu Rev Immunol* 2005, **23**:683-747.
2. Panitch HS, Hirsch RL, Schindler J, Johnson KP: Treatment of multiple sclerosis with gamma interferon: Exacerbations associ-

- ated with activation of the immune function. *Neurology* 1987, **37**:1097-1102.
3. The IFNB Multiple Sclerosis Study Group: Interferon beta-1b is effective in relapsing-remitting multiple sclerosis. I. Clinical results of a multicenter, randomized, double-blind, placebo-controlled trial. *Neurology* 1993, **43**:655-661.
 4. Jacobs LD, Cookfair DL, Rudick RA, Herndon RM, Richert JR, Salazar AM, Fischer JS, Goodkin DE, Granger CV, Simon JH, Alam JJ, Bartoszak DM, Bourdette DN, Braiman J, Brownschidle CM, Coats ME, Cohan SL, Dougherty DS, Kinkel RP, Mass MK, Munschauer FE 3rd, Priore RL, Pullicino PM, Scherokman BJ, Whitham RH, The Multiple Sclerosis Collaborative Research Group (MSCRG): Intramuscular interferon beta-1a for disease progression in relapsing multiple sclerosis. *Ann Neurol* 1996, **39**:285-294.
 5. Jacobs LD, Beck RV, Simon JH, Kinkel RP, Brownschidle CM, Murray TJ, Simonian NA, Slator PJ, Sandrock AV: Intramuscular interferon beta-1a therapy initiated during a first demyelinating event in multiple sclerosis. *CHAMPS Study Group. N Engl J Med* 2000, **343**:898-904.
 6. McRae BL, Semnani RT, Hayes MP, van Seventer GA: Type I IFNs inhibit human dendritic cell IL-12 production and Th1 cell development. *J Immunol* 1998, **160**:4298-4304.
 7. Kozovska ME, Hong J, Zang YC, Li S, Rivera VM, Killian JM, Zhang JZ: Interferon beta induces T-helper 2 immune deviation in MS. *Neurology* 1999, **53**:1692-1697.
 8. Stone LA, Frank JA, Albert PS, Bash C, Smith ME, Maloni H, McFarland HF: The effects of interferon- β on blood-brain barrier disruptions demonstrated by contrast-enhanced magnetic resonance imaging in relapsing-remitting multiple sclerosis. *Ann Neurol* 1995, **37**:611-619.
 9. Satoh J, Paty DW, Kim SU: Differential effects of beta and gamma interferons on expression of major histocompatibility complex antigens and intercellular adhesion molecule-1 in cultured fetal human astrocytes. *Neurology* 1995, **45**:367-373.
 10. Vaubant E, Vukusic S, Gignoux L, Dubief FD, Achiti I, Blanc S, Renoux C, Confavreux C: Clinical characteristics of responders to interferon therapy for relapsing MS. *Neurology* 2003, **61**:184-189.
 11. Rudick RA, Lee JC, Simon J, Ransohoff RM, Fisher E: Defining interferon β response status in multiple sclerosis patients. *Ann Neurol* 2004, **56**:548-555.
 12. Neilley LK, Goodin DS, Goodkin DE, Hauser SL: Side effect profile of interferon beta-1b in MS: Results of an open label trial. *Neurology* 1996, **46**:554-554.
 13. Bielekova B, Martin R: Development of biomarkers in multiple sclerosis. *Brain* 2004, **127**:1463-1478.
 14. Steinman L, Zamvil S: Transcriptional analysis of targets in multiple sclerosis. *Nature Rev Immunol* 2003, **3**:483-492.
 15. Wandinger KP, Strüzebecher CS, Bielekova B, Detore G, Rosenwald A, Staudt LM, McFarland HF, Martin R: Complex immunomodulatory effects of interferon- β in multiple sclerosis include the upregulation of T helper 1-associated marker genes. *Ann Neurol* 2001, **50**:349-357.
 16. Koike F, Satoh J, Miyake S, Yamamoto T, Kawai M, Kikuchi S, Nomura K, Yokoyama K, Ota K, Kanda T, Fukazawa T, Yamamura T: Microarray analysis identifies interferon β -regulated genes in multiple sclerosis. *J Neuroimmunol* 2003, **139**:109-118.
 17. Weinstock-Guttman B, Badgett D, Patrick K, Hartrich L, Santos R, Hall D, Baier M, Feichter J, Ramanathan M: Genomic effects of IFN- β in multiple sclerosis patients. *J Immunol* 2003, **171**:2694-2702.
 18. Satoh J, Nakanishi M, Koike F, Miyake S, Yamamoto T, Kawai M, Kikuchi S, Nomura K, Yokoyama K, Ota K, Kanda T, Fukazawa T, Yamamura T: Microarray analysis identifies an aberrant expression of apoptosis and DNA damage-regulatory genes in multiple sclerosis. *Neurobiol Dis* 2005, **18**:537-550.
 19. van Boxel-Dezaire AH, van Trigt-Hoff SC, Killestein J, Schrijver HM, van Houwelingen JC, Polman CH, Nagelkerken L: Contrasting response to interferon β -1b treatment in relapsing-remitting multiple sclerosis: does baseline interleukin-12p35 messenger RNA predict the efficacy of treatment? *Ann Neurol* 2000, **48**:313-322.
 20. Stürzebecher S, Wandinger KP, Rosenwald A, Sathyamoorthy M, Tzou A, Mattar P, Frank JA, Staudt L, Martin R, McFarland HF: Expression profiling identifies responder and non-responder phenotypes to interferon- β in multiple sclerosis. *Brain* 2003, **126**:1419-1429.
 21. Satoh J, Nakanishi M, Koike F, Onoue H, Aranami T, Yamamoto T, Kawai M, Kikuchi S, Nomura K, Yokoyama K, Ota K, Saito T, Ohta M, Miyake S, Kanda T, Fukazawa T, Yamamura T: T cell gene expression profiling identifies distinct subgroups of Japanese multiple sclerosis patients. *J Neuroimmunol* 2006, **174**:108-118.
 22. Baranzini SE, Mousavi P, Rio J, Caillier SJ, Stillman A, Villoslada P, Wyatt MM, Comabella M, Greller LD, Somogyi R, Montalban X, Oksenberg JR: Transcription-based prediction of response to IFN β using supervised computational methods. *PLoS Biol* 2005, **3**:e2.
 23. Interferon Stimulated Gene Database Arranged into Functional Categories [<http://www.lerner.ccf.org/labs/williams/xchp.html.cgi>]
 24. Theofilopoulos AN, Baccala R, Beutler B, Kono DH: Type I interferons (α/β) in immunity and autoimmunity. *Annu Rev Immunol* 2005, **23**:307-335.
 25. Taniguchi T, Ogasawara K, Takaoka A, Tanaka N: IRF family of transcription factors as regulators of host defense. *Annu Rev Immunol* 2001, **19**:623-655.
 26. Honda K, Yanai H, Negishi H, Asagiri M, Sato M, Mizutani T, Shimada N, Ohba Y, Takaoka A, Yoshida N, Taniguchi T: IRF-7 is the master regulator of type-I interferon-induced immune response. *Nature* 2005, **434**:772-777.
 27. Marx N, Mach F, Sauty A, Leung JH, Sarafi MN, Ransohoff RM, Libby P, Plutzky J, Luster AD: Peroxisome proliferator-activated receptor- γ activators inhibit IFN- γ -induced expression of the T cell-active CXC chemokines IP-10, Mig, and I-TAC in human endothelial cells. *J Immunol* 2000, **164**:6503-6508.
 28. Kim OS, Park EJ, Joe E, Jou I: JAK-STAT signaling mediates gangliosides-induced inflammatory responses in brain microglial cells. *J Biol Chem* 2002, **277**:40594-40601.
 29. Zlotnik A, Yoshie O: Chemokines: a new classification system and their role in immunity. *Immunity* 2000, **12**:121-127.
 30. Balashov KE, Rottman JB, Weiner HL, Hancock WW: CCR5⁺ and CXCR3⁺ T cells are increased in multiple sclerosis and their ligands MIP-1 α and IP-10 are expressed in demyelinating brain lesions. *Proc Natl Acad Sci USA* 1999, **96**:6873-6878.
 31. Sørensen T, Tani M, Jensen J, Pierce V, Lucchinetti C, Folcik VA, Qin S, Rottman J, Sellebjerg F, Strieter RM, Frederiksen JL, Ransohoff RM: Expression of specific chemokines and chemokine receptors in the central nervous system of multiple sclerosis patients. *J Clin Invest* 1999, **103**:807-815.
 32. Simpson JE, Newcombe J, Cuzner ML, Woodroffe MN: Expression of the interferon- γ -inducible chemokines IP-10 and Mig and their receptor, CXCR3, in multiple sclerosis lesions. *Neuropathol Appl Neurobiol* 2000, **26**:133-142.
 33. McManus C, Berman JW, Brett FM, Staunton H, Farrell M, Brosnan CF: MCP-1, MCP-2 and MCP-3 expression in multiple sclerosis lesions: an immunohistochemical and in situ hybridization study. *J Neuroimmunol* 1998, **86**:20-29.
 34. Van Der Voorn P, Tekstra J, Beelen RH, Tensen CP, Van Der Valk P, De Groot CJ: Expression of MCP-1 by reactive astrocytes in demyelinating multiple sclerosis lesions. *Am J Pathol* 1999, **154**:45-51.
 35. Hokeness KL, Kuziel WA, Biron CA, Salazar-Mather TP: Monocyte chemoattractant protein-1 and CCR2 interactions are required for IFN- α/β -induced inflammatory responses and antiviral defense in liver. *J Immunol* 2005, **174**:1549-1556.
 36. Giorelli M, Livrea P, Defazio G, Iacovelli L, Capobianco L, Picascia A, Salles M, Martino D, Aniello MS, Trojano M, De Biasi A: Interferon beta-1a counteracts effects of activation on the expression of G-protein-coupled receptor kinases 2 and 3, β -arrestin-1, and regulators of G-protein signaling 2 and 16 in human mononuclear leukocytes. *Cell Signal* 2002, **14**:673-678.
 37. Reif K, Cyster JG: RGS molecule expression in murine B lymphocytes and ability to down-regulate chemotaxis to lymphoid chemokines. *J Immunol* 2000, **164**:4720-4729.
 38. Der SD, Zhou A, Williams BRG, Silverman RH: Identification of genes differentially regulated by interferon α , β , or γ using oligonucleotide arrays. *Proc Natl Acad Sci USA* 1998, **95**:15623-15628.
 39. Nourbakhsh M, Kälble s, Dörrie A, Hauser H, Resch K, Kracht M: The NF- κ B repressing factor is involved in basal repression and interleukin (IL)-1-induced activation of IL-8 transcrip-

- tion by binding to a conserved NF- κ B-flanking sequence element. *J Biol Chem* 2001, **176**:4501-4508.
40. Lund BT, Ashikian N, Ta HQ, Chakryan Y, Manoukian K, Groshen S, Gilmore W, Cheema GS, Stohl W, Burnett ME, Ko D, Kachuck NJ, Weiner LP: **Increased CXCL8 (IL-8) expression in multiple sclerosis.** *J Neuroimmunol* 2004, **155**:161-171.
 41. Iarlori C, Reale M, De Luca G, Di Iorio A, Feliciani C, Tulli A, Conti P, Gambi D, Lugaresi A: **Interferon β -1b modulates MCP-1 expression and production in relapsing-remitting multiple sclerosis.** *J Neuroimmunol* 2002, **123**:170-179.
 42. Rothuizen LE, Buclin T, Spertini F, Trincharid I, Munafu A, Buchwalder PA, Ythier A, Biollaz J: **Influence of interferon β -1a dose frequency on PBMC cytokine secretion and biological effect markers.** *J Neuroimmunol* 1999, **99**:131-141.
 43. Comabella M, Imitola J, Weiner HL, Khoury SJ: **Interferon- β treatment alters peripheral blood monocytes chemokine production in MS patients.** *J Neuroimmunol* 2002, **126**:205-212.
 44. Dayal AS, Jensen MA, Ledo A, Arnason BG: **Interferon-gamma-secreting cells in multiple sclerosis patients treated with interferon beta-1b.** *Neurology* 1995, **45**:2173-2177.
 45. Martínez-Cáceres EM, Rio J, Barrau M, Durán I, Borrás C, Tintoré M, Montalban X: **Amelioration of flulike symptoms at the onset of interferon β -1b therapy in multiple sclerosis by low-dose oral steroids is related to a decrease in interleukin-6 induction.** *Ann Neurol* 1998, **44**:682-685.
 46. Buttmann M, Merzyn C, Rieckmann P: **Interferon- β induces transient systemic IP-10/CXCL10 chemokine release in patients with multiple sclerosis.** *J Neuroimmunol* 2004, **156**:195-203.
 47. Sarris AH, Esgleyes-Ribot T, Crow M, Broxmeyer HE, Karasavvas N, Pugh W, Grossman D, Deisseroth A, Duvic M: **Cytokine loops involving interferon- γ and IP-10, a cytokine chemotactic for CD4⁺ lymphocytes: an explanation for the epidermotropism of cutaneous T-cell lymphoma.** *Blood* 1995, **86**:651-658.
 48. Marckmann S, Wiesemann E, Hilde R, Trebst C, Stangel M, Windhagen A: **Interferon- β up-regulates the expression of co-stimulatory molecules CD80, CD86 and CD40 on monocytes: significance for treatment of multiple sclerosis.** *Clin Exp Immunol* 2004, **138**:499-506.
 49. Buttmann M, Goebeler M, Toksoy A, Schmid S, Graf W, Berberich-Siebel F, Rieckmann P: **Subcutaneous interferon- β injections in patients with multiple sclerosis initiate inflammatory skin reactions by local chemokine induction.** *J Neuroimmunol* 2005, **168**:175-82.
 50. Islam M, Frye RF, Richards TJ, Sbeitan I, Donnelly SS, Glue P, Agarwala SS, Kirkwood JM: **Differential effect of IFN α -2b on the cytochrome P450 enzyme system: a potential basis of IFN toxicity and its modulation by other drugs.** *Clin Cancer Res* 2002, **8**:2480-2487.
 51. Chawla-Sarkar M, Lindner DJ, Liu YF, Williams BR, Sen GC, Silverman RH, Borden EC: **Apoptosis and interferons: role of interferon-stimulated genes as mediators of apoptosis.** *Apoptosis* 2003, **8**:237-249.
 52. Geiss GK, Carter VS, He Y, Kwiciszewski BK, Holzman T, Korh MJ, et al.: **Gene expression profiling of the cellular transcriptional network regulated by alpha/beta interferon and its partial attenuation by the hepatitis C virus nonstructural 5A protein.** *J Virol* 2003, **77**:6367-6375.
 53. Wandinger KP, Lünemann JD, Wengert O, Bellmann-Strobl J, Aktas O, Weber A, Grundstrom E, Ehrlich S, Wernecke KD, Volk HD, Zipp F: **TNF-related apoptosis inducing ligand (TRAIL) as a potential response marker for interferon-beta treatment in multiple sclerosis.** *Lancet* 2003, **361**:2036-2043.
 54. Wesemann DR, Qin H, Kokorina N, Benveniste EN: **TRADD interacts with STAT1- α and influences interferon- γ signaling.** *Nature Immunol* 2004, **5**:199-207.
 55. Balachandran S, Thomas E, Barber GN: **A FADD-dependent innate immune mechanism in mammalian cells.** *Nature* 2004, **432**:401-405.
 56. Stephanou A, Isenberg DA, Nakajima K, Latchman DS: **Signal transducer and activator of transcription-1 and heat shock factor-1 interact and activate the transcription of the Hsp-70 and Hsp-90 β gene promoter.** *J Biol Chem* 1999, **274**:1723-1728.

Pre-publication history

The pre-publication history for this paper can be accessed here:

<http://www.biomedcentral.com/1471-2377/6/18/prepub>

Publish with **BioMed Central** and every scientist can read your work free of charge

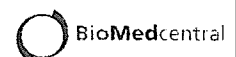
"BioMed Central will be the most significant development for disseminating the results of biomedical research in our lifetime."

Sir Paul Nurse, Cancer Research UK

Your research papers will be:

- available free of charge to the entire biomedical community
- peer reviewed and published immediately upon acceptance
- cited in PubMed and archived on PubMed Central
- yours — you keep the copyright

Submit your manuscript here:
http://www.biomedcentral.com/info/publishing_adv.asp



Selective COX-2 inhibitor celecoxib prevents experimental autoimmune encephalomyelitis through COX-2-independent pathway

Katsuichi Miyamoto,^{1,2} Sachiko Miyake,¹ Miho Mizuno,¹ Nobuyuki Oka,³ Susumu Kusunoki² and Takashi Yamamura¹

¹Department of Immunology, National Institute of Neuroscience, NCNP, Tokyo, ²Department of Neurology, Kinki University School of Medicine, Osaka and ³Department of Rehabilitation Medicine, Minami-kyoto National Hospital, Kyoto, Japan

Correspondence to: Sachiko Miyake, Department of Immunology, National Institute of Neuroscience, NCNP, Kodaira, Tokyo 187-8502, Japan
E-mail: miyake@ncnp.go.jp

Cyclooxygenase (COX) is a key enzyme of arachidonic acid metabolism and exists as two distinct isoforms. COX-1 is constitutively expressed in most tissues, whereas COX-2 is inducibly expressed at the site of inflammation. Selective inhibitors of COX-2 have been developed and have been used as anti-inflammatory agents. Here, we show that a new-generation COX-2 inhibitor, celecoxib, inhibited experimental autoimmune encephalomyelitis (EAE). Celecoxib, but not other COX-2 inhibitors such as nimesulid, prevented myelin oligodendrocyte glycoprotein (MOG) induced EAE when administrated orally on the day of disease induction. Moreover, celecoxib inhibited EAE in COX-2-deficient mice, indicating that celecoxib inhibited EAE in a COX-2-independent manner. In celecoxib-treated mice, interferon- γ (IFN- γ) production from MOG-specific T cells was reduced and MOG-specific IgG1 was elevated compared with vehicle-treated mice. Infiltration of inflammatory cells into the central nervous system and the expression of adhesion molecules, P-selectin and intercellular adhesion molecule-1 (ICAM-1), and a chemokine, monocyte chemoattractant peptide-1 (MCP-1), were inhibited when mice were treated with celecoxib. These results suggest that celecoxib may be useful as a new additional therapeutic agent for multiple sclerosis.

Keywords: COX-2 inhibitor; celecoxib; experimental autoimmune encephalomyelitis; multiple sclerosis

Abbreviations: CMC = carboxymethylcellulose; COX = cyclooxygenase; EAN = experimental autoimmune neuritis; EAE = experimental autoimmune encephalomyelitis; ELISA = enzyme-linked immunosorbent assay; ICAM-1 = intercellular adhesion molecule-1; IFN = interferon; IL = interleukin; LN = lymph node; MCP-1 = monocyte chemoattractant peptide-1; MOG = myelin oligodendrocyte glycoprotein; PBS = phosphate-buffered saline

Received February 6, 2006. Revised April 11, 2006. Accepted May 31, 2006. Advance Access publication July 10, 2006

Introduction

Cyclooxygenase (COX) catalyses the conversion of arachidonic acid to prostaglandins and has two isoforms, COX-1 and COX-2 (Vane *et al.*, 1994; Warner and Mitchell, 2004). COX-1 is constitutively expressed in most tissues and produces prostaglandins involved in maintenance of the gastric mucosa, regulation of renal blood flow and platelet aggregation. On the other hand, COX-2 is inducibly expressed in cells involved in inflammation and in neoplastic tissues by proinflammatory and mitogenic stimuli, and is primarily responsible for the synthesis of prostanoids involved in acute and chronic inflammation (Xie *et al.*, 1997). COX-2

therefore appears to be a suitable target for the anti-inflammatory effects of non-steroidal anti-inflammatory drugs. These findings have provided the rationale for the development of selective inhibitors of COX-2.

Celecoxib is a new generation of highly specific COX-2 inhibitors that have been approved for the treatment of rheumatoid arthritis and other inflammatory diseases. The selectivity of COX-2 inhibition is much higher than traditional COX-2 inhibitors (Penning *et al.*, 1997). Furthermore, celecoxib has been shown to exert a potent anti-tumour effect. Interestingly, the anti-tumour effect by celecoxib

has been reported via both COX-2-dependent and COX-2-independent mechanisms (Grosch *et al.*, 2001). For example, cell cycle arrest and apoptosis of various kinds of cells induced by celecoxib appeared to be COX-2-independent effects (Hsu *et al.*, 2000; Arico *et al.*, 2002; Liu *et al.*, 2004).

Experimental autoimmune encephalomyelitis (EAE) is a widely used animal model for multiple sclerosis that can be induced by immunization with myelin antigens such as myelin oligodendrocyte glycoprotein (MOG). EAE is mediated primarily by CD4⁺ Th1 T cells producing interferon- γ (IFN- γ) and tumour necrosis factor- α (TNF- α) (Nicholson and Kuchroo, 1996; Kumar *et al.*, 1997; Zhang *et al.*, 1997). COX-2 is expressed in neurons and endothelial cells in healthy brain. In rats with EAE, the expression of COX-2 was reported to be upregulated in endothelial cells in inflammatory lesions. In addition, non-selective COX-2 inhibitors have been reported to moderately ameliorate EAE (Prosiegel *et al.*, 1989; Weber *et al.*, 1991; Simmons *et al.*, 1992), suggesting that COX-2 may have an important role in the pathogenesis of EAE (Deininger and Schluesener, 1999). Furthermore, we recently demonstrated that COX-2 inhibitors suppress experimental autoimmune neuritis (EAN), a model of Guillain-Barré syndrome, which is also characterized as a CD4⁺-Th1 T-cell-mediated autoimmune neurological disease model similar to EAE (Miyamoto *et al.*, 1998, 1999, 2002). These findings led us to investigate the effect of COX-2 inhibitors on EAE.

In the present study, we found that celecoxib greatly suppressed EAE in comparison with traditional COX-2 inhibitors. Furthermore, we have demonstrated that celecoxib inhibited EAE by inhibiting Th1 response of autoreactive T cells and that this inhibition was COX-2-independent. Finally, we demonstrated that celecoxib prevented cell entry into the CNS in association with the inhibition of the expression of P-selectin, intercellular adhesion molecule-1 (ICAM-1) and monocyte chemoattractant peptide-1 (MCP-1). These results highlighted the COX-2-independent therapeutic potential of celecoxib for multiple sclerosis.

Material and methods

Mouse

Wild-type C57Bl/6 (B6) mice were purchased from Clea Japan (Tokyo, Japan). COX-2-deficient mice (COX-2^{-/-}) have been backcrossed to B6 background for more than five generations and were purchased from Taconic (Germantown, NY, USA). These mice were maintained under specific pathogen-free conditions.

Induction of EAE

For induction of EAE, mice were immunized (5–10 mice per group) subcutaneously in flanks with 100 μ g of MOG_{35–55} peptide (MEVG-WYRSPFSRVVHLYRNGK) in 0.1 ml phosphate-buffered saline (PBS) and 0.1 ml complete Freund's adjuvant (CFA) containing 1 mg *Mycobacterium tuberculosis* H37Ra (Difco Laboratories, Detroit, MI, USA) and were injected intravenously with 200 ng

of pertussis toxin (List Biological Laboratories, Campbell, CA, USA) on the day of immunization and 2 days later.

Clinical assessment of EAE

EAE was scored on the following scale: 0 = no clinical signs; 1 = partial loss of tail tonicity; 2 = completely limp tail and abnormal gait; 3 = partial hindlimb paralysis; 4 = complete hindlimb paralysis; and 5 = fore- and hindlimb paralysis or moribund state.

Treatment with COX-2 inhibitors

Mice were orally administered 5 μ g/g of COX-2 inhibitor, celecoxib (Searle, St Louis, MO, USA) (Penning *et al.*, 1997), nimesulid (Nakarai Tesque, Kyoto, Japan) (Nakatsuji *et al.*, 1996), or indomethacin (Nakarai Tesque) in 0.5% carboxymethylcellulose (CMC) via a feeding cannula every 2 days. Control mice were orally administered vehicle (0.5% CMC) alone.

Measurement of MOG_{35–55}-specific IgG1 and IgG2a titres

Enzyme-linked immunosorbent assay (ELISA) plates (Sumitomo, Tokyo, Japan) were coated with 10 μ g/ml MOG_{35–55} in PBS overnight at 4°C. After blocking with 2% bovine serum albumin (BSA) in PBS, different dilutions of the serum from animals at Day 30 after immunization, or normal mice or PBS were added to the plate. MOG_{35–55}-specific antibodies were detected using biotin-labelled anti-IgG1 and anti-IgG2a antibodies (Vector Laboratories, Burlingame, CA, USA). After adding streptavidin-peroxidase (BD Biosciences, San Jose, CA, USA) and a substrate, plates were read at OD₄₅₀ values.

MOG_{35–55}-specific T-cell proliferation assay

On Day 11 after immunization with MOG_{35–55}, draining lymph nodes (LN) were harvested and single cell suspensions were prepared. Cells were cultured in RPMI1640 medium (Gibco, Grand Island, NY, USA) supplemented with 5×10^{-5} M 2-mercaptoethanol, 2 mM L-glutamine, 100 U/ml penicillin and streptomycin and 1% autologous mouse serum, and seeded onto 96-well flat-bottom plates (1×10^6 cells/well). The cells were stimulated with peptide for 72 h at 37°C in a humidified air condition with 5% CO₂. To measure cellular proliferation, [³H]-thymidine was added (1 μ Ci/well) and uptake of the radioisotope during the final 18 h of culture was counted with a beta-1205 counter (Pharmacia, Uppsala, Sweden). To evaluate proliferative responses of LN cells to peptide, we determined the Δ c.p.m. value for cells in each well by subtracting the background c.p.m.

Detection of cytokines and chemokine

LN cells from the MOG_{35–55}-immunized mice were cultured in the standard medium in 96-well flat-bottom plates at 1×10^6 /well for 48 h in the presence of the different concentrations of MOG_{35–55}. The concentrations of IFN- γ , interleukin-4 (IL-4) and IL-10 in the supernatants were measured by using a sandwich ELISA following the protocol provided by BD Biosciences. A chemokine, MCP-1, in the serum from mice on Day 7, 10 and 14 after induction of EAE was also measured by using a sandwich ELISA following the protocol provided by BD Biosciences. All reagents, including recombinant mouse cytokines, chemokine and antibodies were purchased from BD Biosciences.

Analysis of infiltrating cells isolated from CNS

Mice were anaesthetized with diethyl ether on Day 14 after induction of EAE. After perfusion with PBS, brain and spinal cord were removed and homogenized. After washing with PBS, mononuclear cells were isolated using Ficoll gradient (Amersham Biosciences, Piscataway, NJ, USA) (Krakowski *et al.*, 1997). The cells were stained with APC-labelled anti-CD3 antibody, fluorescein isothiocyanate (FITC) labelled anti-CD4 or CD8 or CD19 antibody (BD Biosciences) and were analysed by flow cytometer (BD FACS Calibur). Apoptosis of lymphocytes was analysed by using Annexin-5 apoptosis kit (BD Biosciences).

Pathological analysis

The brain and spinal cord were removed on Day 7, 10 and 14 after induction of EAE. Ten-micrometre frozen sections were fixed with acetone and stained with haematoxylin and eosin (HE), Luxol fast blue or antibodies of adhesion molecule ICAM-1 (CD54), vascular cell adhesion molecule-1 (VCAM-1; CD106), E-selectin (CD62E) and P-selectin (CD62P) (BD Biosciences), following the protocol provided by BD Biosciences.

Statistics

For statistic analysis, non-parametric Mann–Whitney *U*-test was used to calculate significant levels for all measurements. Values of $P < 0.05$ were considered statistically significant.

Results

Celecoxib inhibits EAE

To examine the effect of celecoxib on the development of EAE, we first administered celecoxib at the time of immunization with MOG_{35–55}. Oral administration of celecoxib reduced the incidence of disease and suppressed maximum EAE score and cumulative score compared with the control group (Fig. 1A, Table 1). Histological comparison between the thoracic region of the spinal cord demonstrated reduced monocyte infiltration and demyelination in celecoxib-treated mice compared with vehicle-treated mice (Fig. 2A–D). Celecoxib was also effective in reducing the severity of disease when administered at Day 8

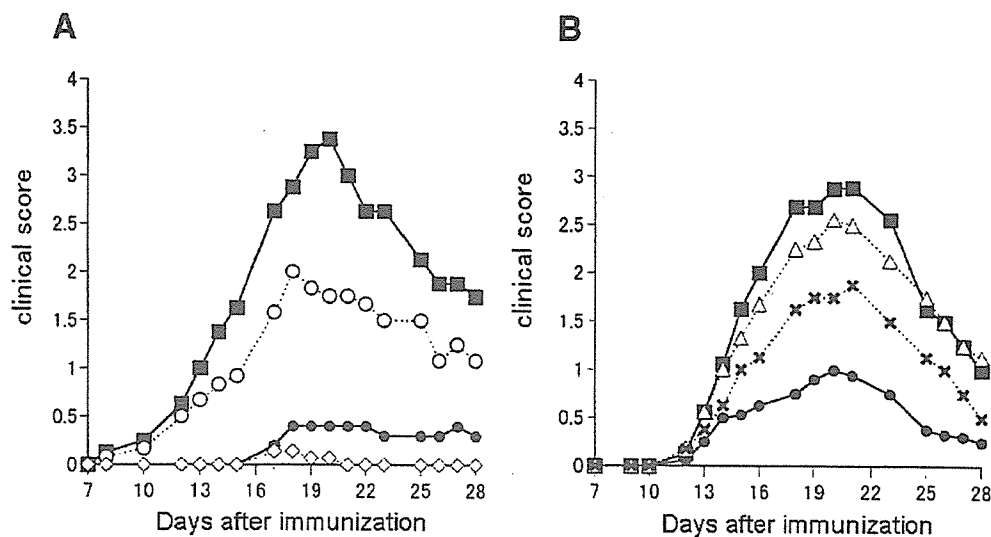


Fig. 1 Effect of celecoxib on actively induced EAE. EAE was induced in female B6 mice by immunization with MOG_{35–55} in CFA as described in Material and methods. (A) Mice were orally administered 5 µg/g (closed circles) or 10 µg/g (open diamond) of celecoxib starting from the day of the immunization, or with 5 µg/g of celecoxib starting from 8 days after the immunization (open circles). Control mice were administered vehicle alone (closed squares). Statistical analysis is shown in Table 1. (B) Mice were orally administered 5 µg/g of celecoxib (closed circles) or nimesulid (open triangle) or indomethacin (crosses) every 2 days from the day of EAE induction. Control mice were administered vehicle alone (closed squares). Statistical analysis is shown in Table 2. One representative experiment of two independent experiments is expressed as mean \pm SEM.

Table 1 Clinical scores of EAE treated with celecoxib

	Max. score	Day of onset	Incidence (%)	Cumulative score
Control (CMC)	3.50 \pm 0.20	12.50 \pm 1.56	100 (10/10)	33.00 \pm 5.05
Celecoxib 10 µg/g	0.14 \pm 0.05*	17.50 \pm 0.50	20.0 (2/10)	0.42 \pm 0.04*
Celecoxib 5 µg/g	0.40 \pm 0.40*	17.00 \pm 0.00	20.0 (2/10)	3.80 \pm 3.80*
Celecoxib 5 µg/g (from Day 8)	2.42 \pm 0.57	14.20 \pm 1.83	83.3 (10/12)	20.17 \pm 5.22

Four groups of mice were immunized with MOG_{35–55} peptide for induction of EAE. The control CMC solution, 5 or 10 µg/g of celecoxib diluted in CMC, was orally injected via a cannula every 2 days starting from Day 0 or 8 after induction of EAE. Mean \pm SEM of the following parameters are shown: maximum score of EAE (Max. score), the days of EAE onset, incidence of paralysed mice among sensitized mice (Incidence) and summation of the clinical scores from Day 0 to 30 (Cumulative score). * $P < 0.05$ versus control.

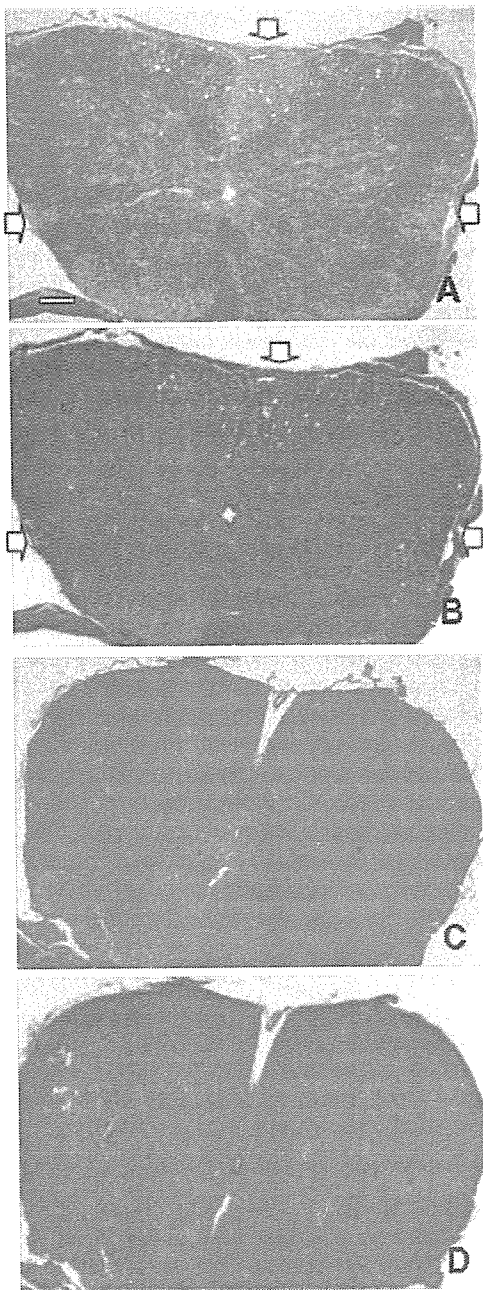


Fig. 2 Histopathological assessment of the CNS region in EAE-induced mice. Brains and spinal cords from EAE mice were removed on Day 14 after immunization as described in Material and methods. Thinly sliced (10 μ m) frozen sections of the brains obtained from vehicle-treated mice (**A** and **B**) or celecoxib-treated mice (**C** and **D**) were stained with haematoxylin and eosin (**B** and **D**), or Luxol fast blue (**A** and **C**).

post-EAE-induction. Although indomethacin suppressed EAE to some extent, all mice died around Day 30 after immunization owing to intestinal ulcer. In contrast, oral administration of nimesulid, another COX-2 inhibitor, did

not suppress either the incidence or the severity of EAE (Fig. 1B). Composite data from experiments is shown in Tables 1 and 2.

Celecoxib inhibits MOG-specific Th1 response

To determine the mechanisms by which celecoxib inhibits EAE, we examined the level of MOG-specific IgG1 and IgG2a in the serum samples collected from individual EAE-induced mice on Day 30. It is generally accepted that elevation of antigen-specific IgG2a antibody results from augmentation of a Th1 immune response to the antigen, whereas a higher level of IgG1 antibody would reflect a stronger Th2 response to the antigen. There was a significant elevation of the level of MOG₃₅₋₅₅-specific IgG1 and a slight reduction in the level of MOG-specific IgG2a in celecoxib-treated group compared with vehicle-treated group (Fig. 3A). In contrast, there was no significant difference in the level of either IgG1 or IgG2a in nimesulid-treated mice compared with vehicle-treated group (Fig. 3B).

To further investigate the response of T cells to MOG₃₅₋₅₅ in celecoxib-treated mice, we examined the proliferative response and cytokine production of draining LN cells *in vitro*. Mice were immunized with MOG₃₅₋₅₅ and were administered celecoxib or vehicle on the day of immunization. Ten days after immunization, draining LN cells were collected and cultured with MOG₃₅₋₅₅ peptide. As shown in Fig. 4A, there was no significant difference in a proliferative response of MOG-reactive T cells between celecoxib-treated and vehicle-treated groups. We next examined the levels of cytokines in the culture supernatant by ELISA. The level of IFN- γ was reduced in the culture supernatants of LN cells obtained from mice treated with celecoxib compared with that from control mice (Fig. 4B). IL-4 and IL-10 were not detected in either culture supernatant. These results indicate that celecoxib reduces Th1 cytokine production from MOG-reactive T cells.

Celecoxib prevents EAE even in COX-2-deficient mice

Since another COX-2 inhibitor, nimesulid, did not have the inhibitory effect on EAE, we examined whether celecoxib could inhibit EAE in COX-2-deficient mice. As shown in Fig. 5A, the maximum EAE score, the day of onset and the severity of EAE were not significantly different between COX-2^{-/-} and wild-type mice. Administration of celecoxib prevented the development of EAE in COX-2^{-/-} mice as well as in wild-type mice. Consistent with the severity of EAE, the levels of MOG-specific IgG1 and IgG2a in COX-2^{-/-} mice were not different compared with wild-type B6 mice (Fig. 5B). Moreover, celecoxib treatment increased the level of MOG-specific IgG1 even in COX-2^{-/-} mice, resulting in the elevation of IgG1 : IgG2a ratio similar to that in wild-type mice (CMC = 0.29, celecoxib = 3.00) and COX-2^{-/-} mice (CMC = 0.42, celecoxib = 2.52). These results indicate that the effect on the inhibition of EAE

Table 2 Clinical scores of EAE treated with celecoxib or other non-steroidal anti-inflammatory drugs

	Max. score	Day of onset	Incidence (%)	Cumulative score	Death (%)
Control (CMC)	3.05 ± 0.20	13.10 ± 1.16	100 (10/10)	26.47 ± 5.13	10 (1/10)
Celecoxib	1.02 ± 0.53*	14.30 ± 1.77	90 (9/10)	7.58 ± 6.72*	0 (0/10)
Nimesulid	2.54 ± 0.68	13.50 ± 1.56	100 (10/10)	22.15 ± 4.75	0 (0/10)
Indomethacin	1.70 ± 0.83	13.90 ± 1.93	100 (10/10)	15.21 ± 3.89	100 (10/10)*

Each mouse was immunized with MOG_{35–55} peptide for induction of EAE. The control CMC solution, or 5 µg/g of drugs diluted in CMC, was orally administered via a cannula every other day. Mean ± SEM of the following parameters are shown: maximum score of EAE (Max. score), the days of EAE onset, incidence of paralyzed mice among sensitized rats (Incidence), summation of the clinical scores from Day 0 to 30 (Cumulative score) and the incidence of death during EAE (Death). **P* < 0.05 versus control.

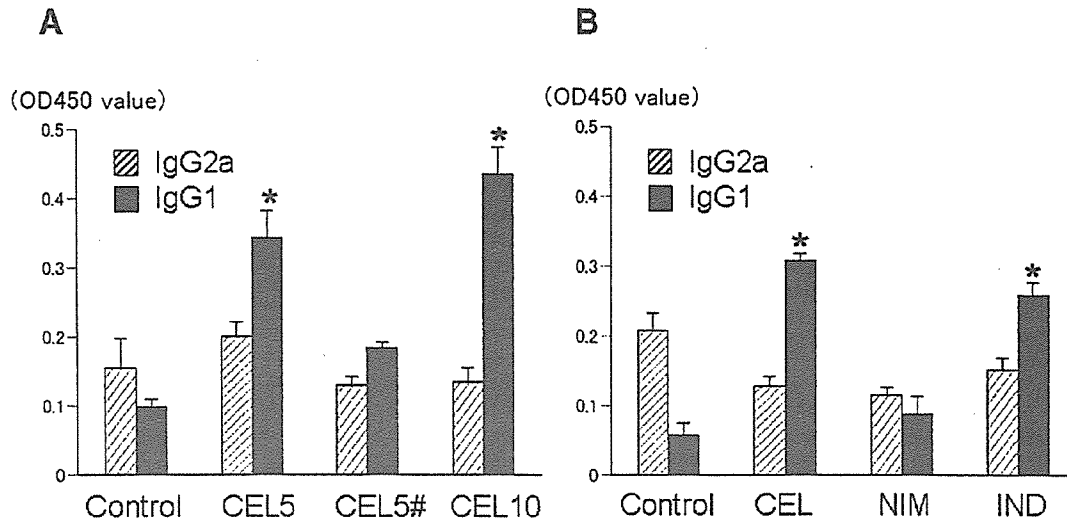


Fig. 3 Analysis of MOG_{35–55} IgG1 and IgG2a in EAE-induced mice. The relative titers of anti-MOG IgG1 and IgG2a in serum samples from individual mice (*n* = 10) on Day 30 after immunization were analysed as indicated in Methods. Data represent mean ± SEM. **P* < 0.05 versus control. (a) Control = vehicle alone, CEL5 = 5 µg/g of celecoxib, CEL5# = 5 µg/g of celecoxib from Day 8 after the immunization, CEL10 = 10 µg/g of celecoxib. (b) Control = vehicle alone, CEL = celecoxib, NIM = nimesulid, IND = indomethacin.

and Th1 response by celecoxib is mediated by a COX-2-independent pathway (Table 3)

Celecoxib inhibits an infiltration of immune cells into CNS

To characterize the infiltrated cells into CNS, we isolated mononuclear cells from CNS obtained from celecoxib-treated or vehicle-treated mice. Mononuclear cells isolated from the CNS of vehicle-treated mice include CD3⁺ T cells that comprised >80% of CD4⁺ cells. In mice treated with celecoxib, the number of infiltrated cells was less than one-seventh compared with vehicle-treated mice (Table 4). In addition, we analysed apoptotic cells from CNS, spleen and draining LNs using annexin-5 staining. There was no difference in the frequency of apoptotic cells in all organs examined from celecoxib-treated and vehicle-treated mice (data not shown). These results suggest that celecoxib inhibits an infiltration of inflammatory cells into the CNS rather than induction of apoptosis of autoreactive T cells.

Celecoxib suppresses the expression of adhesion molecules and a chemokine related to cell infiltration into CNS

For the recruitment of autoreactive T cells into the brain through the blood–brain barrier (BBB), some adhesion molecules such as ICAM-1, VCAM-1 and P-selectin, and chemokines such as MCP-1 are required (Engelhardt *et al.*, 1997; Hofmann *et al.*, 2002). We performed an immunohistostaining of sliced brain sections from mice with EAE using antibodies against adhesion molecules. ICAM-1, VCAM-1 and P-selectin (Fig. 6A, C and E) were expressed on choroid plexus in the brain obtained from EAE-induced mice. In contrast, in brains obtained from celecoxib-treated mice, the expression level of P-selectin and ICAM-1 was lower compared with the control (Fig. 6B, D and F). In addition, we examined the level of MCP-1, which is an important chemokine involved in recruiting autoreactive T cells into the brain. As shown in Table 5, the level of MCP-1 in the serum obtained from

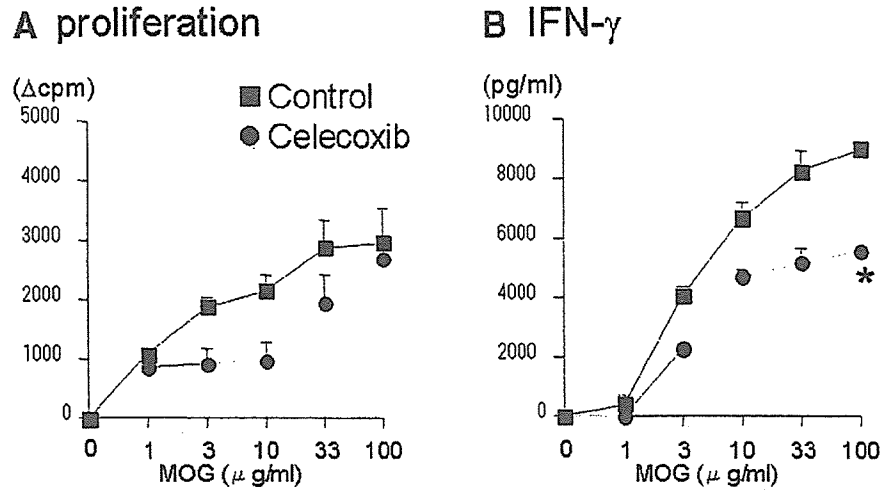


Fig. 4 Comparison of MOG_{35–55}-specific T-cell response after treatment with celecoxib. Popliteal and inguinal LN cells from treated and control animals were incubated in the presence of MOG_{35–55} for 48 h. Proliferative response was determined by the uptake of [³H] thymidine (A), and IFN- γ was detected by ELISA (B). Representative data of two independent experiments are shown ($n = 5$ for each group). Error bars represent SEM. * $P < 0.05$ versus control.

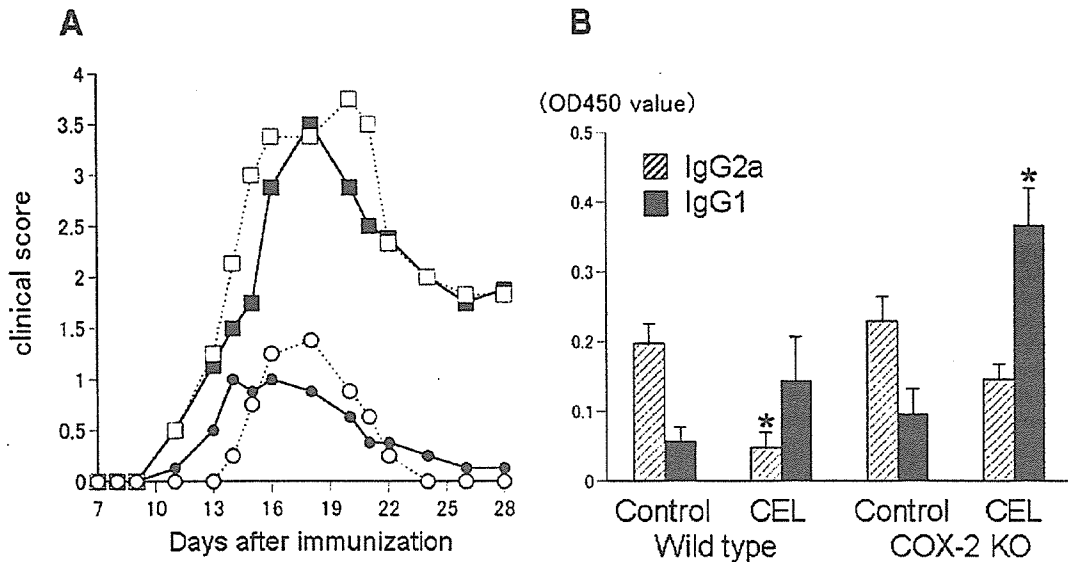


Fig. 5 Effect of celecoxib on actively induced EAE in COX-2-deficient mice. B6 mice and COX-2-deficient mice were immunized with MOG_{35–55} in CFA as described in Material and methods. (A) Mice were orally administered celecoxib (5 μ g/g) every 2 days starting from the day of the immunization. Statistical analysis is shown in Table 3. Closed squares = vehicle alone for wild-type mice; closed circles = 5 μ g/g of celecoxib for wild-type mice, open squares = vehicle alone for COX-2-deficient mice, open circles = 5 μ g/g of celecoxib for COX-2-deficient mice. (B) The relative titres of anti-MOG IgG1 and IgG2a in serum samples from individual mice on Day 30 after immunization were analysed as indicated in Material and methods. Data represent mean \pm SEM. * $P < 0.05$ versus control. Control = vehicle alone, CEL = celecoxib. One representative experiment of two independent experiments is expressed as mean \pm SEM.

celecoxib-treated mice was significantly lower compared with that obtained from vehicle-treated mice. These findings suggested that celecoxib inhibits an infiltration of immune-mediated cells into CNS through the BBB by suppression of P-selectin, ICAM-1 and MCP-1.

Discussion

In the present study, we have demonstrated that a new-generation selective COX-2 inhibitor, celecoxib, strongly inhibited the development of EAE as compared with vehicle treatment or a traditional COX-2 inhibitor, nimesulid. The

Table 3 Clinical scores of EAE in COX-2-deficient mice

Mouse	Treatment	Max. score	Day of onset	Incidence (%)	Cumulative score
Wild-type	CMC	3.54 ± 0.28	12.60 ± 1.15	100 (10/10)	24.85 ± 6.37
	Celecoxib	1.13 ± 0.39*	13.20 ± 1.80	80 (8/10)	6.29 ± 4.02*
COX-2 ^{-/-}	CMC	3.75 ± 0.44	12.78 ± 1.57	100 (8/8)	29.88 ± 5.62
	Celecoxib	1.46 ± 0.51*	14.13 ± 1.96	87.5 (7/8)	5.39 ± 3.36*

Wild-type and COX-2^{-/-} mice were immunized with MOG_{35–55} peptide to induce EAE. The control CMC solution, or 5 µg/g of celecoxib diluted in CMC, was administered every other day. Mean ± SEM of the following parameters are shown: maximum score of EAE (Max. score), the days of EAE onset, incidence of paralysed mice among sensitized mice (Incidence) and summation of the clinical scores from Day 0 to 30 (Cumulative score). **P* < 0.05 versus control.

Table 4 Cell infiltration into the CNS of EAE-induced mice

	Mononuclear cell	CD3 ⁺ cell	CD4 ⁺ cell	CD19 ⁺ cell
EAE mice				
Control (CMC)	667 ± 176	203 ± 69	158 ± 50	6 ± 1
Celecoxib	90 ± 57*	12 ± 8*	9 ± 5*	0 ± 0
Naive mice	20 ± 6	5 ± 2	3 ± 2	1 ± 0

CNS tissues from each group mouse were homogenized on Day 18 after immunization with MOG_{35–55} peptide. Mononuclear cells were isolated by Percoll solution. The cells were stained with cell markers and analysed by flow cytometer. Mean ± SEM of cell number (10³ cells/mouse) is shown. Representative data of two independent experiments are shown (*n* = 5 for each group). **P* < 0.05 versus control.

inhibitory effect on EAE by celecoxib was also evident in COX-2-deficient mice, indicating that celecoxib suppressed EAE in a COX-2-independent mechanism. In celecoxib-treated mice, MOG-specific Th1 responses were reduced and infiltration of immune cells was significantly inhibited compared with vehicle-treated mice, which were associated with lower expression of ICAM-1 and P-selectin on the choroid plexus in the brain.

Since EAE is an autoimmune inflammatory disease, administering COX-2 inhibitor was expected to inhibit disease as well as other COX inhibitors. Recently, Muthian *et al.* (2006) showed that some COX-2 inhibitors such as NS398 and LM01 suppressed EAE, when administered intraperitoneally every other day. In our study, we could not observe the inhibitory effect of nimesulid on EAE when orally administered every 2 days using the same conditions in which celecoxib exhibited a strong inhibitory effect. The route and timing of administration might be critical to modulate diseases. The inhibitory effect mediated by celecoxib was stronger compared with other COX inhibitors, suggesting that different mechanisms may be occurring in addition to the suppression of production of prostanoids that occurred at sites of disease and inflammation. In fact, COX-2 was not required for the celecoxib-mediated inhibitory effect on EAE. Recent studies have suggested that COX-2-independent pathways may contribute to celecoxib-mediated anti-tumour or anti-arthritis effect through enhanced apoptosis of tumour cells or synovial cells (Kusunoki *et al.*, 2002;

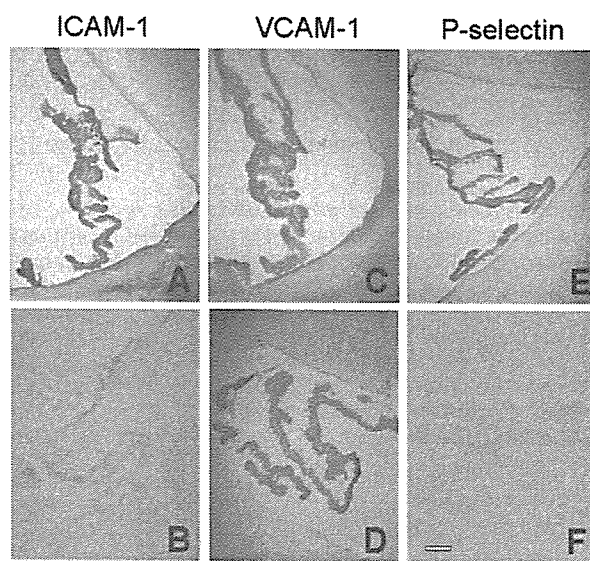


Fig. 6 Immunohistochemical staining with ICAM-1, VCAM-1 and P-selectin of the brain in EAE-induced mice. Brains from EAE mice were removed on Day 14 after immunization as described in Material and methods. Thinly sliced (10 µm) frozen sections of the brain were immunostained with anti-ICAM-1 antibody (A and B), anti-VCAM-1 antibody (C and D) and anti-P-selectin antibody (E and F). Figure shows choroid plexus region. Bar = 100 µm.

Shishodia *et al.*, 2004). In our study, enhancing apoptosis of immune cells was not detected, indicating that different COX-2-independent mechanisms might be important for celecoxib-mediated inhibition of EAE. We observed that celecoxib treatment inhibited Th1 responses of MOG-reactive T cells. In the regulation of Th1/Th2 responses, prostaglandin E2 synthesized by COX has been reported to suppress IL-2 and IFN-γ production by a Th1 clone (Snijdwint *et al.*, 1993). In addition, Meyer *et al.* (2003) reported that administration of COX-2 inhibitor, NS398, increased *Helicobacter*-stimulated IL-12 and IFN-γ production, suggesting that COX-2 inhibition resulted in enhanced Th1 responses. In contrast, celecoxib inhibited Th1 responses of autoreactive T cells. Therefore, this COX-2-independent effect on immune system may be a mechanism to explain why celecoxib suppresses EAE to a greater degree compared with that of other COX-2 inhibitors. Allonza *et al.* (2006) reported that

Table 5 Serum level of MCP-1 in EAE mice after treatment with celecoxib

	Day 0	Day 7	Day 10	Day 14
EAE mice				
Control (CMC) (n = 18)	ND	60.0 ± 21.0	42.6 ± 17.0	ND
Celecoxib (n = 16)	ND	8.5 ± 5.0*	12.9 ± 8.5	ND
Naive mice (n = 10)	ND	ND	ND	ND

B6 mice were immunized with MOG_{35–55} peptide as described in Material and methods. Serum samples from individual mice were collected on Day 0, 7, 10 and 14 after immunization. Serum concentration of MCP-1 was measured by ELISA. Data represent mean ± SEM (pg/ml). ND = not detectable. *P < 0.05 versus control.

celecoxib inhibits IL-12 $\alpha\beta$ and $\beta 2$ folding and secretion in association with the increased interaction of IL-12 with calreticulin, an endoplasmic reticulum-resident chaperone in retention of misfolded cargo proteins, while blocking interaction with Erp44. They also demonstrated that an analogue of celecoxib lacking the COX-2 inhibitor activity showed identical effects to that of celecoxib on folding and secretion of IL-12, indicating that the effect is COX-2-independent. Since IL-12 is a key cytokine to provoke Th1 immune response, reduction in MOG-specific Th1 response is consistent with these previous findings.

The infiltration of immune cells in the CNS was significantly inhibited in celecoxib-treated mice. Celecoxib has been reported to reduce expression of P-selectin and ICAM-1 in experimental inflammatory models such as experimental colitis (Cuzzocrea *et al.*, 2001, 2002). In our study, we observed that celecoxib suppressed expression of P-selectin and ICAM-1 in the brain of EAE mice. Since P-selectin and ICAM-1 are the adhesion molecules involved in the recruitment of inflammatory cells into CNS (Engelhardt *et al.*, 1997; Dietrich, 2002; Scott *et al.*, 2004), inhibition of cellular infiltration by celecoxib might be mediated by the downregulation of the expression of adhesion molecules.

Chemokines are also required for recruitment of immune cells into the CNS. MCP-1 is reported to be an essential chemokine in EAE (Hofmann *et al.*, 2002). In the mouse model of atherosclerosis, Wang *et al.* (2005) reported that celecoxib decreased the inflammatory response and hyperplasia following vascular injury through inhibition of MCP-1 induction. We detected a decreased level of MCP-1 in the serum in celecoxib-treated mice on EAE. The suppression of MCP-1 by celecoxib might also contribute to the reduction of infiltrating cells into the CNS.

In conclusion, celecoxib has a potent therapeutic potential for EAE by inducing a Th2 bias and suppressing infiltration of inflammatory cells into the CNS through a COX-2-independent mechanism. Further analysis of celecoxib-mediated suppression of EAE will help drug development for multiple sclerosis. Celecoxib is hoped to be a new choice of the treatment of multiple sclerosis.

Acknowledgement

This study was supported by the Japan Research Foundation for Clinical Pharmacology.

References

- Alloza I, Baxter A, Chen Q, Matthiesen R, Vanderbroeck K. Celecoxib inhibits interleukin-12 $\alpha\beta$ and $\beta 2$ folding and secretion by a novel COX-2-independent mechanism involving chaperones of the endoplasmic reticulum. *Mol Pharm* 2006; 69: 1579–87.
- Arico S, Pattingre S, Bauvy C, Gane P, Barbat A, Codogno P, *et al.* Celecoxib induces apoptosis by inhibiting 3-phosphoinositide-dependent protein kinase-1 activity in the human colon cancer HT-29 cell line. *J Biol Chem* 2002; 277: 27613–21.
- Cuzzocrea S, Mazzone E, Serrano I, Dugo L, Centorrino T, Ciccolo A, *et al.* Celecoxib, a selective cyclo-oxygenase-2 inhibitor reduces the severity of experimental colitis induced by dinitrobenzene sulfonic acid in rats. *Eur J Pharmacol* 2001; 431: 91–102.
- Cuzzocrea S, Mazzone E, Sautelin L, Dugo L, Serrano I, De Sarro A, *et al.* Protective effects of celecoxib on lung injury and red blood cells modification induced by carrageenan in the rat. *Biochem Pharmacol* 2002; 63: 785–95.
- Deininger MH, Schluesener HJ. Cyclooxygenases-1 and -2 are differentially localized to microglia and endothelium in rat EAE and glioma. *J Neuroimmunol* 1999; 95: 202–8.
- Dietrich JB. The adhesion molecule ICAM-1 and its regulation in relation with the blood-brain barrier. *J Neuroimmunol* 2002; 128: 58–68.
- Engelhardt B, Vestweber D, Hallmann R, Schulz M. E- and P-selectin are not involved in the recruitment of inflammatory cells across the blood-brain barrier in experimental autoimmune encephalomyelitis. *Blood* 1997; 90: 4459–72.
- Grosch S, Tegeder I, Niederberger E, Brautigam L, Geisslinger G. COX-2 independent induction of cell cycle arrest and apoptosis in colon cancer cells by the selective COX-2 inhibitor celecoxib. *FASEB J* 2001; 15: 2742–4.
- Hofmann N, Lachnit N, Streppel M, Witter B, Neiss WF, Guntinas-Lichius O, *et al.* Increased expression of ICAM-1, VCAM-1, MCP-1, and MIP-1 alpha by spinal perivascular macrophages during experimental allergic encephalomyelitis in rats. *BMC Immunol* 2002; 6: 11.
- Hsu AL, Ching TT, Wang DS, Song X, Rangnekar VM, Chen CS. The cyclooxygenase-2 inhibitor celecoxib induces apoptosis by blocking Akt activation in human prostate cancer cells independently of Bcl-2. *J Biol Chem* 2000; 275: 11397–403.
- Krakowski ML, Owens T. The central nervous system environment controls effector CD4+ T cell cytokine profile in experimental allergic encephalomyelitis. *Eur J Immunol* 1997; 27: 2840–7.
- Kumar V, Aziz F, Sercarz E, Miller A. Regulatory T cells specific for the same framework 3 region of the Vb8.2 chain are involved in the control of collagen II-induced arthritis and experimental autoimmune encephalomyelitis. *J Exp Med* 1997; 185: 1725–33.
- Kusumoki N, Yamazaki R, Kawai S. Induction of apoptosis in rheumatoid synovial fibroblasts by celecoxib, but not by other selective cyclooxygenase 2 inhibitors. *Arthritis Rheum* 2002; 46: 3159–67.
- Liu X, Yue P, Zhou Z, Khuri FR, Sun SY. Death receptor regulation and celecoxib-induced apoptosis in human lung cancer cells. *J Natl Cancer Inst* 2004; 96: 1769–80.
- Meyer F, Ramanujam KS, Gobert AP, James SP, Wilson KT. Cutting edge: cyclooxygenase-2 activation suppresses Th1 polarization in response to *Helicobacter pylori*. *J Immunol* 2003; 171: 3913–7.
- Miyamoto K, Oka N, Kawasaki T, Satoh H, Akiguchi I, Kimura J. The effect of cyclooxygenase-2 inhibitor on experimental allergic neuritis. *Neuroreport* 1998; 9: 2331–4.
- Miyamoto K, Oka N, Kawasaki T, Satoh H, Matsuo A, Akiguchi I. The action mechanism of cyclooxygenase-2 inhibitor for treatment of experimental allergic neuritis. *Muscle Nerve* 1999; 22: 1704–9.
- Miyamoto K, Oka N, Kawasaki T, Miyake S, Yamamura T, Akiguchi I. New cyclooxygenase-2 inhibitor for treatment of experimental autoimmune neuritis. *Muscle Nerve* 2002; 25: 280–2.

- Muthian G, Raikwar HP, Johnson C, Rajasingh J, Kalgutkar A, Marnett LJ, et al. COX-2 inhibitors modulate IL-12 signaling through JAK-STAT pathway leading to Th1 response in experimental allergic encephalomyelitis. *J Clin Immunol* 2006; 26: 73–85.
- Nakatsui S, Terada N, Yoshimura T, Horie Y, Furukawa M. Effects of nimesulide, a preferential cyclooxygenase-2 inhibitor, on carrageenan-induced pleurisy and stress-induced gastric lesions in rats. *Prostaglandins* 1996; 55: 395–402.
- Nicholson LB, Kuchroo VK. Manipulation of the Th1/Th2 balance in autoimmune disease. *Curr Opin Immunol* 1996; 8: 837–42.
- Penning TD, Talley JJ, Bertenshaw SR, Carter JS, Collins PW, Docter S, et al. Synthesis and biological evaluation of the 1,5-diarylpyrazole class of cyclooxygenase-2 inhibitors: identification of 4-[5-(4-methylphenyl)-3-(trifluoromethyl)-1H-pyrazol-1-yl]benzene sulfonamide (SC-58635, celecoxib). *J Med Chem* 1997; 40: 1347–65.
- Prosiegel M, Neu I, Mallinger J, Wildfeuer A, Mehler L, Vogl S, et al. Suppression of experimental autoimmune encephalomyelitis by dual cyclooxygenase and 5-lipoxygenase inhibition. *Acta Neurol Scand* 1989; 79: 223–6.
- Scott GS, Kean RB, Fabis MJ, Mikheeva T, Brimer CM, Phares TW, et al. ICAM-1 upregulation in the spinal cords of PLS1J mice with experimental allergic encephalomyelitis is dependent upon TNF- α production triggered by the loss of blood-brain barrier integrity. *J Neuroimmunol* 2004; 155: 32–42.
- Shishodia S, Koul D, Aggarwal BB. Cyclooxygenase (COX)-2 inhibitor celecoxib abrogates TNF-induced NF- κ B activation through inhibition of activation of I κ B kinase and Akt in human non-small cell lung carcinoma: correlation with suppression of COX-2 synthesis. *J Immunol* 2004; 173: 2011–22.
- Simmons RD, Hugh AR, Willenborg DO, Cowden WB. Suppression of active but not passive autoimmune encephalomyelitis by dual cyclo-oxygenase and 5-lipoxygenase inhibition. *Acta Neurol Scand* 1992; 85: 197–9.
- Snijdewint F, Kalinski P, Wierenga E, Bos J, Kapasenberg M. Prostaglandin E2 differentially modulate cytokine secretion profiles of human T helper lymphocytes. *J Immunol* 1993; 150: 5321.
- Vane JR, Mitchell JA, Appleton I, Tomlinson A, Bishop-Bailey D, Croxtall J, et al. Inducible isoforms of cyclooxygenase and nitric oxide synthase in inflammation. *Proc Natl Acad Sci USA* 1994; 91: 2046–50.
- Wang K, Tarakji K, Zhou Z, Zhang M, Forudi F, Zhou X, et al. Celecoxib, a selective cyclooxygenase-2 inhibitor, decreases monocyte chemoattractant protein-1 expression and neointimal hyperplasia in the rabbit atherosclerotic balloon injury model. *J Cardiovasc Pharmacol* 2005; 45: 61–7.
- Warner TD, Mitchell JA. Cyclooxygenases: new forms, new inhibitors, and lessons from the clinic. *FASEB J* 2004; 18: 790–804.
- Weber F, Meyermann R, Hempel K. Experimental allergic encephalomyelitis: prophylactic and therapeutic treatment with the cyclooxygenase inhibitor piroxicam (Feldene). *Int Arch Allergy Appl Immunol* 1991; 95: 136–41.
- Xie WL, Chipman JG, Robertson DL, Erikson RL, Simmons DL. Expression of a mitogen-responsive gene encoding prostaglandin synthase is regulated by mRNA splicing. *Proc Natl Acad Sci USA* 1991; 88: 2692–6.
- Zhang B, Yamamura T, Kondo T, Fujiwara M, Tabira T. Regulation of experimental autoimmune encephalomyelitis by natural killer (NK) cells. *J Exp Med* 1997; 186: 1677–87.

Invariant V α 19i T cells regulate autoimmune inflammation

J Ludovic Croxford¹, Sachiko Miyake¹, Yi-Ying Huang², Michio Shimamura² & Takashi Yamamura¹

T cells expressing an invariant V α 19-J α 33 T cell receptor α -chain (V α 19i TCR) are restricted by the nonpolymorphic major histocompatibility complex class Ib molecule MR1. Whether V α 19i T cells are involved in autoimmunity is not understood. Here we demonstrate that T cells expressing the V α 19i TCR transgene inhibited the induction and progression of experimental autoimmune encephalomyelitis (EAE), a mouse model of multiple sclerosis. Similarly, EAE was exacerbated in MR1-deficient mice, which lack V α 19i T cells. EAE suppression was accompanied by reduced production of inflammatory mediators and increased secretion of interleukin 10. Interleukin 10 production occurred at least in part through interactions between B cells and V α 19i T cells mediated by the ICOS costimulatory molecule. These results suggest an immunoregulatory function for V α 19i T cells.

Two distinct mouse T cell subsets express invariant TCR α chains: V α 14-J α 18 (V α 14i; ref. 1) and V α 19-J α 33 (V α 19i; ref. 2). Although conventional T cells recognize peptide antigens presented by polymorphic major histocompatibility complex class Ia molecules, V α 14i 'invariant' T cell populations recognize nonpeptide antigens^{3,4} presented in the context of the nonpolymorphic major histocompatibility complex class Ib molecule CD1d. MR1 may be able to present glycolipids *in vitro* to V α 19i T cells⁵, but the identity or type of endogenous ligand recognized by V α 19i T cells *in vivo* is unknown. However, antigen recognition is essential for the development of T cells expressing V α 14i and V α 19i TCR chains, as these subsets are absent from *Cd1d1^{-/-}* and *Mri1^{-/-}* mice, respectively^{6,7}. Similar invariant T cell subsets are present in humans^{8,9}. Many of these cells also express natural killer (NK) cell markers on their surface (such as mouse NK1.1). Consequently, CD1d-restricted invariant T cells have traditionally been referred to as 'NKT cells' (V α 14i NKT cells)¹⁰.

Transgenic overexpression of the V α 14i TCR chain protects against the development of mouse models of type 1 diabetes¹¹ and multiple sclerosis¹², suggesting that V α 14i NKT cells may be involved in regulating autoimmunity. In addition, susceptibility to type 1 diabetes is linked to quantitative and functional deficiencies in V α 14i NKT cells¹³. Mechanistic studies suggest that V α 14i NKT cells may down regulate autoimmunity by increasing the production of T helper type 2 (T_H2) cytokines¹⁴⁻¹⁹. However, in other conditions, NKT cells may promote the exacerbation of autoimmune disease. V α 14i NKT cell-deficient mice show ameliorated arthritis compared with that of their wild-type counterparts^{18,20,21}.

The immune function of MR1-restricted invariant T cells remains less clear than that of CD1d-restricted lymphocytes. MR1-restricted invariant T cells were first identified among human peripheral blood

CD4⁺CD8⁻ T cells as a clonally expanded population expressing an invariant V α 7.2-J α 33 TCR chain (V α 7.2i T cells)²². Subsequent studies identified clonally expanded T cells expressing the highly homologous invariant V α 19-J α 33 TCR chain in mice and cattle⁹. V α 19i T cell development has been found to depend on the nonpolymorphic major histocompatibility complex class Ib molecule MR1 and on the presence of B cells⁷. The V α 19i TCR is uniquely overexpressed in the gut lamina propria and V α 19i T cell development depends on the presence of commensal gut flora, indicating potential involvement of these cells in gut immunity^{2,7}. As MR1 molecules are thought to be retained in the endoplasmic reticulum, intestinal flora might provide exogenous ligands for the V α 19i TCR, or a cellular 'stress' signal, that enables transit of MR1 from the endoplasmic reticulum to the cell surface^{2,7}.

Human V α 7.2i T cells² but not mouse gut V α 19i T cells express NKT cell markers⁷. In contrast, the V α 19i TCR is expressed by most T cell hybridomas derived from liver NK1.1⁺ T cells from *Cd1d1^{-/-}* mice²³. Furthermore, 25–50% of V α 19i cells from V α 19i transgenic mice on a *Tcra^{-/-}* background express NK1.1 (ref. 24). Those divergent results regarding NK1.1 expression remain unclear, but may be due to differences among mouse genetic backgrounds. Alternatively, as with CD1d-restricted T cells, a subpopulation of MR1-restricted T cells may lack NK1.1 expression. Based on their predominant distribution in the gut, MR1-restricted T cells are often referred to as 'mucosal-associated invariant T cells'^{2,7}. To avoid confusion, we subsequently use the term 'V α 19i T cells' to describe V α 19i T cells expressing NK1.1.

The V α 7.2i TCR is over-represented in central nervous system (CNS) lesions from multiple sclerosis autopsy samples²⁵, whereas the V α 24i TCR is mostly absent²⁶. Those findings led us to speculate that MR1-restricted T cells may 'preferentially' migrate to CNS lesions,

¹Department of Immunology, National Institute of Neuroscience, National Centre of Neurology and Psychiatry, Tokyo 187-8502, Japan. ²Developmental Immunology Unit, Mitsubishi Kagaku Institute of Life Sciences, Tokyo 194-8511, Japan. Correspondence should be addressed to T.Y. (yamamura@ncnp.go.jp).

Received 26 May; accepted 5 July; published online 30 July 2006; doi:10.1038/ni1370

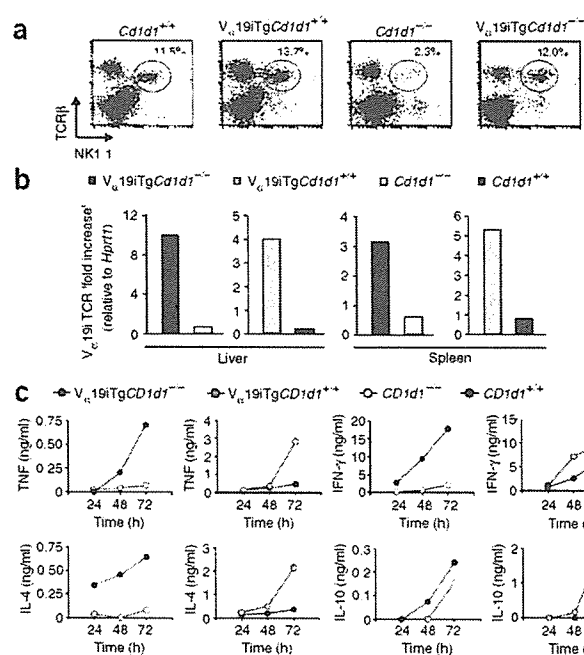


Figure 1 Characterization of NK1.1⁺ T cells from V_α19i Tg mice. (a) Flow cytometry of liver NK1.1⁺ T cells 48 h after anti-asialo-GM1-mediated depletion of NK cells (mouse genotypes, above plots). Numbers above gated regions indicate the percentage of NK1.1⁺TCRβ⁺ cells. (b) Real-time RT-PCR of V_α19i TCR mRNA expression in liver or spleen NK1.1⁺ T cells (mouse genotypes, key). Data are presented as 'fold increase' over expression of *Hprt1*. (c) Cytokines in the supernatants of sorted liver NK1.1⁺ T cells (mouse genotypes, key) stimulated by immobilized anti-CD3 *in vitro*, measured at 24, 48 and 72 h after stimulation. Data are representative of two separate experiments (a,b) or the mean of two replicate values from two separate experiments (c).

where they regulate CNS inflammation. We designed this study to address the function of MR1-restricted T cells in experimental autoimmune encephalomyelitis (EAE)^{14,17}, a mouse model of multiple sclerosis. Here we report that over-representation of V_α19i T cells decreased the severity of EAE, whereas depletion of V_α19i T cells exacerbated EAE. Furthermore, V_α19i T cells exerted an influence on the phenotype and functions of autoimmune T cells in the draining lymph nodes and spleens of mice. In particular, over-representation of V_α19i T cells reduced the production of proinflammatory cytokines and increased the production of interleukin 10 (IL-10), which may account for V_α19i T cell-mediated suppression of autoimmune disease. Finally, interactions between V_α19i T cells and B cells mediated by the ICOS costimulatory molecule increased B cell IL-10 production and may therefore represent a mechanism by which V_α19i T cells regulate inflammation.

RESULTS

Characterization of transgenic V_α19i T cells

An antibody specific for the V_α19i TCR chain does not exist, and wild-type mice have very few MR1-restricted V_α19i T cells. Therefore, to circumvent those experimental hurdles and to evaluate the function of V_α19i T cells *in vivo*, we used V_α19i TCR-transgenic (V_α19i Tg) mice⁵, which were originally generated by injection into C57BL/6 mouse oocytes of a transgenic construct encoding a V_α19-J_α33 TCR construct driven by the endogenous *Tcrα* promoter. We crossed the transgenic line with *Cd1d1*^{+/+} and *Cd1d1*^{-/-} C57BL/6 mice for seven to nine generations. First we compared numbers of liver NK1.1⁺ T cells present in *Cd1d1*^{+/+}, *Cd1d1*^{-/-}, V_α19i Tg *Cd1d1*^{+/+} and V_α19i Tg *Cd1d1*^{-/-} mice (Fig. 1a). TCRβ⁺NK1.1⁺ T cells comprised 11.5% of total liver lymphocytes in *Cd1d1*^{+/+} mice but only 2.3% of total liver lymphocytes in *Cd1d1*^{-/-} mice. Therefore, most (about 80%) of NK1.1⁺ T cells in *Cd1d1*^{+/+} mice corresponded to CD1d-restricted V_α14i NKT cells, whereas about 20% were probably MR1-restricted²³. Notably, V_α19i Tg *Cd1d1*^{-/-} mice had many NK1.1⁺ T cells (12.0%), indicating that overexpression of the V_α19i TCR in *Cd1d1*^{-/-} mice compensated for the reduction in NK1.1⁺ T cells

caused by CD1d deficiency. In contrast, the number of NK1.1⁺ T cells was only slightly higher in V_α19i Tg *Cd1d1*^{+/+} mice, which had normal numbers of V_α14i NKT cells. To confirm that the NK1.1⁺ T cell population in V_α19i Tg mice was enriched in cells expressing the V_α19i TCR chain, we measured V_α19i mRNA transcripts in NK1.1⁺ liver cells and splenocytes by real-time RT-PCR (Fig. 1b). V_α19i mRNA expression was much greater in liver and splenic NK1.1⁺ T cell populations from V_α19i Tg *Cd1d1*^{+/+} or V_α19i Tg *Cd1d1*^{-/-} mice than in those from nontransgenic littermates (Fig. 1b). In V_α19i T cells, the V_α19i TCR chain 'preferentially' associates with TCRβ chains containing Vβ8 or Vβ6 segments²⁴. Approximately 60–70% of liver NKT cells from V_α19i Tg *Cd1d1*^{-/-} or V_α19i Tg *Tcrα*^{-/-} mice expressed either Vβ8 or Vβ6, compared with 30–40% of conventional T cells in the same mice (unpublished observations). These observations collectively demonstrate that NK1.1⁺ T cell populations in V_α19i Tg mice are highly enriched in cells expressing V_α19-J_α33 TCR chains and Vβ6 or Vβ8 TCR chains. Next we compared the ability of NK1.1⁺ T cells from V_α19i Tg and nontransgenic mice to produce immunosuppressive cytokines. To obtain V_α19i T cells, we depleted V_α19i Tg *Cd1d1*^{-/-} mice of NK cells by injecting antibody to

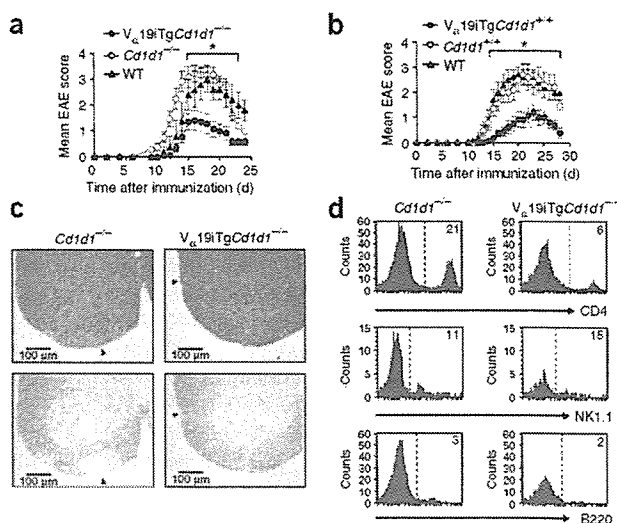


Figure 2 V_α19i T cells in EAE. (a,b) Clinical EAE scores of mice immunized with MOG(35–55). WT, wild-type. Data represent mean score ± s.e.m. from three independent experiments ($n = 10–22$ mice). (c) Monocyte infiltration and demyelination (arrowheads) of the lumbar spinal cord during EAE (day 15). (d) Quantification of spinal cord cellular infiltrates by flow cytometry. Areas to the right of dashed lines indicate positive cellular staining; numbers in histograms indicate percentage of CD4⁺, NK1.1⁺ (gated on CD3⁺) or B220⁺ cells. *, $P < 0.05$ (Mann-Whitney U-test). Data are representative of three separate experiments.



Table 1 $V_{\alpha}19i$ T cells in EAE

Group	Mice with EAE	Group score	EAE score	Day of onset
Wild-type	10 of 10	3.3 ± 0.3	3.3 ± 0.3	13.6 ± 0.7
<i>Cd1d1</i> ^{-/-}	18 of 18	3.4 ± 0.2	3.4 ± 0.2	11.7 ± 0.5
$V_{\alpha}19i$ Tg <i>Cd1d1</i> ^{-/-}	13 of 22	1.3 ± 0.3***	2.2 ± 0.2**	14.3 ± 0.6**
Wild-type	7 of 7	3.6 ± 0.2	3.6 ± 0.2	13.6 ± 0.5
<i>Cd1d1</i> ^{+/-}	11 of 11	3.3 ± 0.4	3.3 ± 0.4	14.8 ± 0.7
$V_{\alpha}19i$ Tg <i>Cd1d1</i> ^{+/-}	9 of 13	1.3 ± 0.3**	1.9 ± 0.4*	18.6 ± 1.2**
NK1.1 ⁻ AdTx	10 of 10	3.6 ± 0.3	3.6 ± 0.3	11.6 ± 0.5
$V_{\alpha}19i$ AdTx	8 of 10	2.2 ± 0.4*	2.8 ± 0.3	15.8 ± 0.6***
<i>Mr1</i> ^{+/-}	10 of 10	3.0 ± 0.2	3.0 ± 0.2	13.9 ± 0.5
<i>Mr1</i> ^{-/-}	8 of 8	4.0 ± 0.0**	4.0 ± 0.0*	11.5 ± 0.5***

Clinical outcome of mice immunized with MOG(35–55) to induce EAE. Data represent number of mice with EAE (of total mice in group); mean group EAE score (± s.e.m.); mean EAE score excluding mice without evidence of EAE (± s.e.m.); and mean day of onset (± s.e.m.). In one experiment, mice received adoptive transfer (AdTx) of $V_{\alpha}19i$ T cells or NK1.1⁻ cells as a control. *, $P < 0.05$, **, $P < 0.01$, and ***, $P < 0.001$, compared with control groups (Mann-Whitney U nonparametric test).

asialo-GM1 (anti-asialo-GM1). We then sorted NK1.1⁺ cells from the liver. When activated by plate-bound anti-CD3, NK1.1⁺ T cells from *Cd1d1*^{+/-} mice secreted more interferon- γ (IFN- γ), tumor necrosis factor (TNF) and interleukin 4 (IL-4) than did those from *Cd1d1*^{-/-} mice, confirming that CD1d-restricted T cells are a chief source of cytokines (Fig. 1c). However, NK1.1⁺ T cells from $V_{\alpha}19i$ Tg mice secreted more TH1 cytokines (IFN- γ and TNF) and TH2 cytokines (IL-4 and IL-10) than did NK1.1⁺ T cells from nontransgenic littermates (Fig. 1c). During subsequent experiments, we used $V_{\alpha}19i$ Tg*Cd1d1*^{-/-} mice as a source of $V_{\alpha}19i$ T cells.

$V_{\alpha}19i$ T cells in EAE

To determine if an abundance of $V_{\alpha}19i$ T cells could modulate autoimmune disease, we analyzed the development and progression of EAE in $V_{\alpha}19i$ Tg mice. We induced EAE by immunizing mice with a

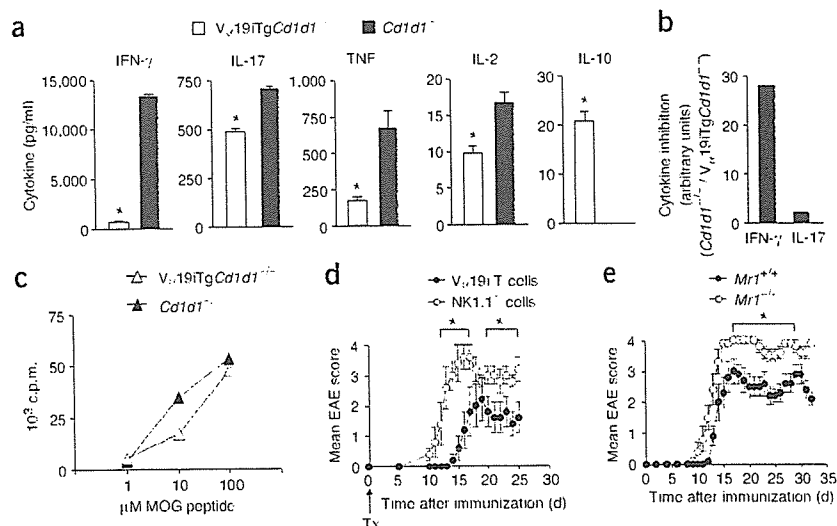
peptide of amino acids 35–55 of myelin oligodendrocyte glycoprotein (MOG(35–55)). The presence of the $V_{\alpha}19i$ transgene suppressed the development and progression of EAE, regardless of whether CD1d-restricted NKT cells were present (Fig. 2a,b and Table 1). The onset of EAE was delayed in $V_{\alpha}19i$ Tg mice, and the incidence and severity of clinical EAE was reduced.

Histological examination of the lumbar (L3) region of the spinal cord 15 d after EAE induction showed less monocyte infiltration and demyelination (assessed by luxol fast blue staining) in $V_{\alpha}19i$ Tg*Cd1d1*^{-/-} mice than in *Cd1d1*^{-/-} mice (Fig. 2c). In agreement with the histology, spinal cords of *Cd1d1*^{-/-} mice contained three times more infiltrating cells than did those from $V_{\alpha}19i$ Tg*Cd1d1*^{-/-} mice (0.09×10^6 and 0.03×10^6 cells respectively, pooled from three mice). Flow cytometry showed fewer CD4⁺ T cells infiltrating the CNS at an active stage of EAE (day 15) in $V_{\alpha}19i$ Tg*Cd1d1*^{-/-} mice (6%) than in nontransgenic littermates (21%; Fig. 2d). Moreover, 11% and 15% of CNS-infiltrating CD3⁺ T cells expressed NK1.1⁺ in *Cd1d1*^{-/-} and $V_{\alpha}19i$ Tg*Cd1d1*^{-/-} mice, respectively, and NK1.1⁺ T cells comprised between 1% and 2% of total CNS-infiltrating cells (Fig. 2d). Also, few B cells trafficked into the CNS during EAE (3% and 2% in *Cd1d1*^{-/-} and $V_{\alpha}19i$ Tg*Cd1d1*^{-/-}, respectively, Fig. 2d). To determine potential mechanisms of reduced CNS infiltration, we analyzed the expression of chemokine receptors and adhesion molecules necessary for T cell migration into the CNS. TCR β ⁺CD4⁺ T cells isolated from the CNS, lymph nodes and spleens of $V_{\alpha}19i$ Tg*Cd1d1*^{-/-} and *Cd1d1*^{-/-} mice on day 18 after EAE induction had similar surface expression of CCR1 and CCR2 (data not shown). However, $V_{\alpha}19i$ Tg*Cd1d1*^{-/-} mice had fewer CD44⁺ and CD49d⁺ TCR β ⁺ splenocytes than did *Cd1d1*^{-/-} mice (Supplementary Fig. 1 online).

Next we examined recall responses of MOG(35–55)-primed T cells by *ex vivo* rechallenge with MOG(35–55) on day 10 after disease induction. Compared with nontransgenic cells, lymph node cells from MOG(35–55)-primed $V_{\alpha}19i$ Tg*Cd1d1*^{-/-} mice produced less pro-inflammatory cytokines (IFN- γ , TNF, IL-2 and IL-17) and more immunosuppressive IL-10 ($P < 0.05$; Fig. 3a). IL-4 and IL-5 were below the limits of analysis detection (less than 5 pg/ml).



Figure 3 Inhibition of EAE is associated with decreased TH1 cytokine production. (a) Cytometric bead assay of cytokines in the supernatants of MOG-specific lymph node cells (1×10^6) isolated from mice on day 10 after EAE induction and rechallenged with 100 μ M MOG(35–55) *in vitro*, measured 72 h after rechallenge. Data represent the mean ± s.e.m. of duplicate samples from three separate experiments. *, $P < 0.05$ (two-tailed Student's *t*-test). (b) Inhibition of IFN- γ or IL-17 in $V_{\alpha}19i$ Tg*Cd1d1*^{-/-} mice versus *Cd1d1*^{-/-} mice from a, presented as 'fold inhibition' of cytokine, calculated as the cytokine concentration from *Cd1d1*^{-/-} mice divided by the cytokine concentration from $V_{\alpha}19i$ Tg*Cd1d1*^{-/-} mice. (c) T cell proliferation of cell preparations identical to those in a from lymph nodes (mouse genotypes, key) rechallenged for 72 h with varying doses of MOG(35–55), assessed by [³H]thymidine incorporation. Data represent the mean of triplicate samples from three separate experiments. (d) Clinical EAE scores of wild-type nontransgenic mice ($n = 10$) that received 1×10^6 sorted $V_{\alpha}19i$ T cells or an equal number of NK1.1⁻ TCR β ⁺ liver cells from $V_{\alpha}19i$ Tg*Cd1d1*^{-/-} mice on the day of immunization with MOG(35–55). Tx indicates the day of adoptive transfer of cells. (e) Clinical EAE scores of *Mr1*^{-/-} and *Mr1*^{+/-} mice ($n = 8–10$) immunized with MOG(35–55). Data are representative of triplicate samples from three separate experiments.



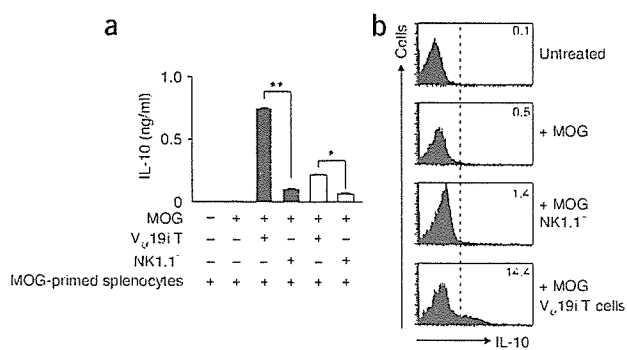


Figure 4 Interactions of V_α19i T cells and splenocytes induce IL-10. (a) Cytometric bead assay of IL-10 in the supernatants of liver V_α19i T cells from naive V_α19i TgCd1d1^{-/-} mice, cultured for 72 h with MOG(35–55)-specific splenocytes and MOG(35–55) (filled bars). In some cases, V_α19i T cells were separated from splenocytes by transwell inserts (open bars). Controls received NK1.1⁻ liver cells from V_α19i TgCd1d1^{-/-} mice. Data represent ± s.e.m. from duplicate samples from three independent experiments. *, $P < 0.01$, and **, $P < 0.001$, compared with control (two-tailed Student's *t*-test). (b) Intracellular flow cytometry of IL-10 production by total cells from a. Areas to the right of dashed lines indicate positive cellular staining; numbers in histograms indicate percentages of IL-10-producing cells. Data are representative of three separate experiments.

IFN- γ secretion was more susceptible to the inhibitory effects of V_α19i T cells than was IL-17 (Fig. 3b). Splenocytes acted like lymph node cells (data not shown).

Overexpression of the V_α19i TCR might compromise the ability of conventional T cells to recognize myelin-derived peptides. However, the proliferative responses of MOG(35–55)-reactive T cells were not lower in V_α19i TgCd1d1^{-/-} mice, despite the inhibition of T_H1 cytokine production (Fig. 3c). Therefore, it is unlikely that the degree of EAE suppression seen in V_α19i TgCd1d1^{-/-} mice was the result of alterations in the MOG(35–55)-specific T cell repertoire. However, to exclude that possibility, we did adoptive transfer experiments. We transferred 1×10^6 V_α19i T cells isolated from V_α19i TgCd1d1^{-/-} mice into nontransgenic mice on the day of EAE induction. Mice that received TCR β^+ T cells were significantly protected from EAE (Fig. 3d) and the onset of clinical disease was significantly delayed (Table 1) compared with that of mice that received V_α19i⁻ NK1.1⁻ T cells.

Next we sought to determine if V_α19i T cell deficiency could also influence clinical EAE. As no V_α19i-specific TCR antibody is available to deplete mice of V_α19i T cells *in vivo*, we used *Mr1*^{-/-} mice, which lack V_α19i T cells⁷. As wild-type nontransgenic mice have about four times more V_α14i NKT cells than V_α19i T cells and *Cd1d1*^{-/-} mice did not show protection from EAE (Fig. 2a), we sought to determine whether the deletion of small numbers of MR1-restricted T cells could alter the clinical course of EAE. Compared with wild-type nontransgenic controls, *Mr1*^{-/-} mice showed a significantly more severe form of EAE with an earlier onset ($P < 0.05$; Fig. 3e and Table 1). Furthermore, T cells from *Mr1*^{-/-} mice proliferated more and produced more T_H1 cytokines and less IL-10 (data not shown). These experiments collectively suggest that V_α19i T cells have a regulatory function in a T_H1-mediated autoimmune disease.

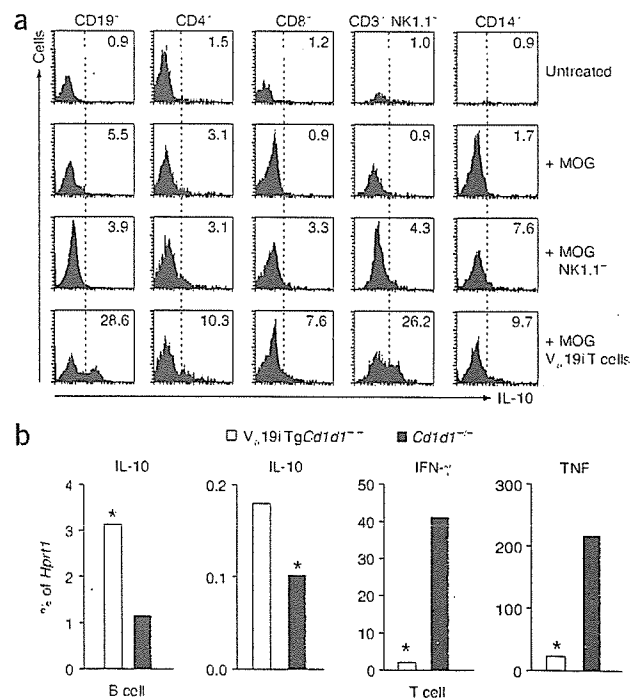
V_α19i T cells induce B cell IL-10 production

MOG(35–55)-primed V_α19i Tg lymph node cells and splenocytes secreted IL-10, which potently inhibits EAE^{27–30} (Fig. 3a). Therefore, we sought to determine whether an increase in V_α19i T cells augmented general IL-10 production. To address that, we developed

Figure 5 V_α19i T cells induce B cells to secrete IL-10. (a) Intracellular flow cytometry of IL-10 production by liver V_α19i T cells from naive V_α19i TgCd1d1^{-/-} mice, cultured for 72 h with MOG(35–55)-specific splenocytes and MOG(35–55). Areas to the right of dashed lines indicate positive cellular staining; numbers in histograms indicate percentage of IL-10-producing cells expressing various surface markers (above plots). Data are representative of two separate experiments. (b) Real-time RT-PCR of the expression of transcripts encoding various cytokines (above graphs) by splenic CD19⁺ B cells or CD4⁺ T cells sorted from mice with EAE. Data are expressed as a percentage of expression of *Hprt1* and are representative of two separate experiments. *, $P < 0.05$ (two-tailed Student's *t*-test).

a mixed-lymphocyte assay in which we cultured NK1.1⁺ or NK1.1⁻ T cells from V_α19i TgCd1d1^{-/-} mice together with MOG(35–55)-primed nontransgenic splenocytes (Fig. 4a). Neither NK1.1⁺ or NK1.1⁻ T cells inhibited the proliferation of MOG(35–55)-primed splenic T cells restimulated with MOG(35–55) (data not shown). Cytokine analysis showed that the coculture supernatant contained considerable IL-10 (after stimulation with MOG(35–55)) in the presence of NK1.1⁺ but not NK1.1⁻ T cells from V_α19i TgCd1d1^{-/-} mice (Fig. 4a). NK1.1⁺ T cells from V_α19i TgCd1d1^{-/-} mice induced IL-10 production even in the absence of MOG(35–55) ($P < 0.05$; Supplementary Fig. 2 online). However, IL-10 secretion was significantly enhanced in the presence of exogenous MOG(35–55) ($P < 0.01$; Supplementary Fig. 2). Intracellular cytokine analysis confirmed that IL-10 production was induced by the addition of NK1.1⁺ but not NK1.1⁻ T cells from V_α19i TgCd1d1^{-/-} mice (Fig. 4b). However, in the presence of transwell inserts, IL-10 production was inhibited, indicating that V_α19i T cell-mediated IL-10 production depends mainly on cell-cell contact (Fig. 4a). IL-4 and IL-5 were below the limit of detection (less than 5 pg/ml), and IFN- γ and TNF were slightly upregulated in the presence of V_α19i T cells (data not shown).

To determine which cells produced IL-10, in the same coculture experiment we analyzed IL-10 production by CD19⁺, CD4⁺, CD8⁺,



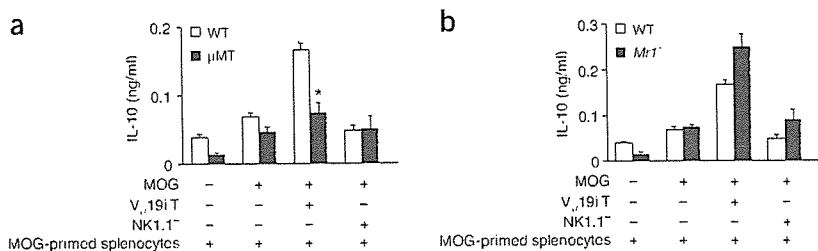


Figure 6 V_α19i T cell-induced IL-10 production is partially B cell dependent but completely MR1 independent. Cytometric bead assay of IL-10 in the supernatants of liver V_α19i T cells from naive V_α19iTgCd1d1^{-/-} mice, cultured for 72 h with MOG(35–55) plus MOG(35–55)-specific splenocytes from wild-type nontransgenic or B cell-deficient μMT mice (a) or from wild-type nontransgenic or MR1-deficient mice (b). Data represent mean ± s.e.m. of duplicate samples from three independent experiments. *, P < 0.05, compared with control (two-tailed Student's *t*-test).

CD3⁺NK1.1⁺ or CD14⁺ cells using intracellular cytokine flow cytometry. The addition of V_α19i T cells greatly increased IL-10 production by CD19⁺ B cells and CD3⁺ NK1.1⁺ NKT cells (Fig. 5a). CD4⁺ and CD8⁺ T cells also showed slight increases in IL-10 production in the presence of V_α19i T cells. To demonstrate that B cells were the main IL-10 producing cells *in vivo*, we extracted RNA from sorted splenic CD4⁺ T cells or CD19⁺ B cells from V_α19iTgCd1d1^{-/-} or nontransgenic mice with EAE (Fig. 5b). In agreement with the results of the *in vitro* coculture system, we found that B cells isolated from V_α19iTgCd1d1^{-/-} mice had higher expression of mRNA transcripts encoding IL-10 than did T cells (Fig. 5b). In addition, B cells from V_α19iTgCd1d1^{-/-} mice had higher expression of *Il10* transcripts than did B cells from Cd1d1^{-/-} mice (Fig. 5b). In contrast, CD4⁺ T cells from V_α19iTgCd1d1^{-/-} mice had lower expression of T_H1 cytokine-encoding mRNA transcripts than did CD4⁺ T cells from Cd1d1^{-/-} mice (Fig. 5b).

To determine if V_α19i T cell–B cell interactions are essential for IL-10 production in the coculture system, we immunized B cell-deficient (μMT) mice with MOG(35–55) to obtain a source of MOG-primed spleen cells lacking B cells. After culture together with V_α19i T cells, B cell-deficient splenocytes produced less IL-10 than did wild-type nontransgenic splenocytes (Fig. 6a). As μMT knockout mice may have unusual follicular architecture, to exclude potential indirect effects we repeated these coculture experiments using B cell-depleted wild-type nontransgenic splenocyte samples. B cell-depleted splenocyte samples produced less IL-10 than did nondepleted splenocyte samples whereas the readdition of wild-type B cells to B cell-depleted splenocyte samples restored IL-10 production (56.3 ± 1.2 pg/ml for

B cell-depleted splenocyte samples; 126.0 ± 4.4 pg/ml for B cell-depleted splenocyte samples with B cells 'added back'; and 170.4 ± 0.8 pg/ml for nondepleted splenocyte samples).

We hypothesized that an interaction between MR1 on B cells and the V_α19i TCR on T cells could induce IL-10 secretion from both cell types. To test that, we immunized Mr1^{-/-} mice with MOG(35–55), followed by coculture experiments. In the absence of MR1, V_α19i T cell-mediated IL-10 production was not reduced (Fig. 6b). These results suggest that V_α19i T cell-induced IL-10 production can occur at least in part through MR1-independent interaction with B cells.

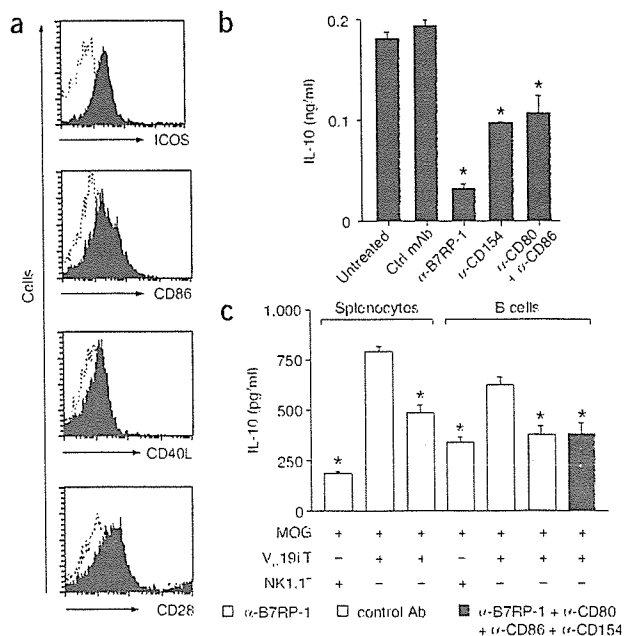
However, non-B cells also seem to contribute to V_α19i T cell-induced IL-10 production.

Costimulation in V_α19i T cell-induced IL-10 production

Naive V_α19i T cells from V_α19iTgCd1d1^{-/-} mice expressed more of the costimulatory molecules CD278 (ICOS), CD86 (B7-2), CD154 (CD40L) and CD28 than did naive splenic T cells (Fig. 7a). V_α19i T cells also expressed CD44 more 'brightly' than did naive T cells (data not shown). These results indicate that V_α19i T cells have an activated or memory phenotype, similar to that of V_α14i NKT cells¹ and 'mucosal-associated invariant T cells' isolated from gut mucosa².

Given that MR1 is not required for IL-10 production, we hypothesized that costimulatory interactions may provide the stimulus for IL-10 production. To test that, we repeated the coculture experiments in the presence of blocking antibodies specific for the costimulatory molecules B7RP-1, CD80, CD86 and CD40L. We found that blockade of each costimulatory pathway resulted in significantly lower IL-10 secretion than that of control cocultures treated with control immunoglobulin (Fig. 7b). However, blockade of the ICOS–B7RP-1 pathway inhibited IL-10 production most substantially. To extend those

Figure 7 ICOS–B7RP-1 costimulation contributes to V_α19i T cell-induced B cell IL-10 production. (a) Flow cytometry of costimulatory molecule expression on the surface of liver V_α19i T cells (filled histograms) and naive splenic T cells from C57BU/6 mice (dotted lines). Data are representative of three separate experiments. (b) Cytometric bead assay of IL-10 in the supernatants of liver V_α19i T cells from naive mice, cultured with MOG(35–55) and MOG(35–55)-specific splenocytes from wild-type nontransgenic EAE mice in the presence of isotype-matched control antibody (Ctrl mAb) or of blocking antibodies specific to various costimulatory molecules (α-; below graph), measured after 72 h of incubation. Data are representative of two separate experiments. (c) Cytometric bead assay of IL-10 in the supernatants of liver V_α19i T cells from naive V_α19iTgCd1d1^{-/-} mice, cultured with MOG(35–55) and MOG(35–55)-specific splenocytes or sorted B cells from wild-type nontransgenic EAE mice in the presence of various antibodies (key), measured after 72 h of incubation. *, P < 0.001, compared with control groups (analysis of variance). Data represent mean ± s.e.m. of triplicate samples from two separate experiments.



© 2006 Nature Publishing Group http://www.nature.com/natureimmunology

findings further, we cultured $V_{\alpha}19i$ T cells together with purified B cells. This resulted in B7RP-1-dependent IL-10 production (Fig. 7c). B7RP-1 blockade partially inhibited IL-10 production in cocultures of $V_{\alpha}19i$ T cells and splenocytes and fully inhibited IL-10 production in cocultures of $V_{\alpha}19i$ T cells and purified B cells (Fig. 7c). These results suggest that although B cells are a chief producer of IL-10 in this system, other cell types also contribute to $V_{\alpha}19i$ T cell-induced IL-10 production. Furthermore, the ICOS–B7RP-1 pathway is vital for $V_{\alpha}19i$ T cell-induced, B cell-mediated IL-10 production, as blockade with a combination of antibodies to costimulatory molecules (B7RP-1, CD80, CD86 and CD40L) inhibited IL-10 to the same degree as anti-B7RP-1 alone (Fig. 7c). However, other costimulatory molecules are involved in $V_{\alpha}19i$ T cell-induced IL-10 production from whole splenocytes (Fig. 7b).

DISCUSSION

Although T cells expressing the invariant $V_{\alpha}19-J_{\alpha}33$ TCR chain were first identified in 1993 (ref. 22), knowledge of the immunological function of this invariant T cell population is still limited. Nevertheless, important characteristics of this lymphocyte subset have been characterized, including their restriction by MR1, their TAP (transporter associated with antigen processing)–independent development in rodents, humans and cattle, and the notable interspecies conservation of this invariant TCR. Because CD1d-restricted $V_{\alpha}14i$ NKT cells, which influence autoimmunity, have similar properties, we speculated that MR1-restricted T cells would also be capable of modifying autoimmunity. However, $V_{\alpha}19i$ T cells are distinct from $V_{\alpha}14i$ CD1d-restricted T cells in their 'preferential' distribution in the gut mucosa and their dependence on the presence of B cells and gut flora.

$V_{\alpha}7.2i$ T cells, the human homolog of $V_{\alpha}19i$ T cells, are present in lesions of patients with multiple sclerosis²⁵. As multiple sclerosis is a demyelinating disease involving autoimmune T cells, B cells, macrophages and various inflammatory mediators, it is possible that MR1-restricted T cells may regulate ongoing disease activity in the CNS. Using an animal model of multiple sclerosis, we examined the effect of overexpression or deletion of MR1-restricted T cells on disease course and severity. Our study suggests that $V_{\alpha}19i$ T cells can suppress autoimmune inflammation. In addition, we have shown that $V_{\alpha}19i$ T cells have a memory or activated surface phenotype and are able to produce large amounts of T_H1 and T_H2 cytokines. $NK1.1^+$ T cells from $V_{\alpha}19i$ Tg mice produced more cytokines than did $NK1.1^+$ T cells from $V_{\alpha}19i$ Tg $Cd1d1^{-/-}$ mice, indicating a possible interaction between CD1d- and MR1-restricted lymphocytes.

We undertook several approaches to determine whether $V_{\alpha}19i$ T cells regulate EAE pathogenesis. Overexpression of $V_{\alpha}19i$ T cells protected mice from clinical EAE. Inhibition of EAE was associated with reduced infiltration and demyelination of the spinal cord as well as a decrease in the production of disease-promoting T_H1 cytokines in the draining lymph nodes and spleen and a reciprocal increase in IL-10, a well established inhibitor of EAE^{27–30}. IL-17-secreting cells, which function independently of T_H1 cells, may promote EAE³¹. Here we determined that the inhibitory effect of $V_{\alpha}19i$ T cells is biased toward prevention of secretion of T_H1 cytokines rather than IL-17.

A potential limitation of TCR-transgenic models is the possible disruption of conventional TCR diversity, which could skew TCR recognition of MOG. However, this is unlikely, as anti-MOG T cell proliferative responses were similar in wild-type nontransgenic and $V_{\alpha}19i$ Tg mice. Furthermore, we adoptively transferred liver $V_{\alpha}19i$ T cells from naive $V_{\alpha}19i$ Tg $Cd1d1^{-/-}$ mice into wild-type nontransgenic mice with EAE, which express natural TCR diversity. In those experiments, $V_{\alpha}19i$ T cells effectively inhibited EAE, suggesting that

$V_{\alpha}19i$ T cells have a regulatory function during EAE. However, a potential limitation of our model is the difficulty of obtaining pure $V_{\alpha}19i$ T cell preparations because of the lack of a $V_{\alpha}19$ TCR-specific antibody. Therefore, experiments using sorted $CD3^+$ $NK1.1^+$ cells from $V_{\alpha}19i$ Tg $Cd1d1^{-/-}$ mice may also contain small numbers of non- $V_{\alpha}14i$ TCR $NK1.1^+$ T cells of other TCR specificities. To ascertain whether normal numbers of $V_{\alpha}19i$ T cells in wild-type nontransgenic mice could be involved during EAE, we induced EAE in $Mr1^{-/-}$ mice and found that the absence of $V_{\alpha}19i$ T cells resulted in a more severe clinical disease than that of wild-type nontransgenic mice.

$V_{\alpha}19i$ T cells most likely exert their main effects in the peripheral lymphoid tissue, as the reduction in proinflammatory cytokines and increase in IL-10 was in the draining lymph nodes and spleen. We also demonstrated that the protective effect of $V_{\alpha}19i$ T cells was independent of $V_{\alpha}14i$ NKT cells by using $V_{\alpha}19i$ Tg mice on a CD1d-deficient background. Notably, we found reduced adhesion molecule expression on effector T cells from $V_{\alpha}19i$ Tg $Cd1d1^{-/-}$ mice, which correlated with reduced T cell infiltration of the CNS. However, we did not note low numbers of $V_{\alpha}19i$ T cells ($CD3^+$ $NK1.1^+$ from $V_{\alpha}19i$ Tg $Cd1d1^{-/-}$ mice) and B cells in the CNS of mice with EAE, suggesting that $V_{\alpha}19i$ T cells may also regulate EAE in the CNS.

Coculture experiments suggested that IL-10-producing B cells are involved in the amelioration of EAE in $V_{\alpha}19i$ Tg $Cd1d1^{-/-}$ mice. Notably, that finding is consistent with published studies demonstrating that IL-10-producing B cells are involved in spontaneous remission from EAE and could limit clinical disease when adoptively transferred into mice with EAE³² or a model of collagen-induced arthritis³³. However, those results do not exclude the possibility that *in vivo*, other cell types are also involved in $V_{\alpha}19i$ T cell-mediated immune regulation. B cells express MR1 (ref. 34), and $V_{\alpha}19i$ T cells are MR1 restricted⁷, but IL-10 production was unaffected in coculture experiments with lymphocytes from MR1-deficient mice, suggesting that MR1, although necessary for $V_{\alpha}19i$ T cell selection, is not essential for $V_{\alpha}19i$ T cell-induced B cell IL-10 production.

T cell activation requires TCR stimulation as well as costimulatory signals. Many costimulatory molecules that regulate cell activation and cytokine secretion have been identified: ICOS and its ligand B7RP-1, CD40-CD40L and CD28-CD80 and CD28-CD86 (refs. 35–38). ICOS costimulation induces IL-10 production as well as help for B cell maturation and CD40L expression^{39,40}. The expression of costimulatory molecules on $V_{\alpha}19i$ T cells was unknown before; we have demonstrated here that $V_{\alpha}19i$ T cells express ICOS, CD28, CD86 and CD40L. To determine the contribution of each of these costimulatory signaling pathways on the production of IL-10 after $V_{\alpha}19i$ T cell–B cell interactions, we repeated the coculture experiments using blocking monoclonal antibody to each of the costimulatory pathways. We found that blockade of the ICOS–B7RP-1 pathway inhibited IL-10 production. Furthermore, blockade of the CD40-CD40L, CD28-CD80 or CD28-CD86 pathway also blocked IL-10 production, although not to the extent seen with ICOS blockade.

Commensal flora in the gut are important for the selection of $V_{\alpha}19i$ T cells⁷. $V_{\alpha}19i$ T cells may also control gut production of immunoglobulin A from B cells, suggesting involvement of $V_{\alpha}19i$ T cells in intestinal B cell regulation⁷. Additionally, IL-10 is important for inhibiting excessive inflammation toward gut flora⁴¹, and it has been shown that IL-10 and transforming growth factor- β are involved in immunoglobulin A synthesis and secretion⁴². In the presence of IL-10 and CD40-CD40L signaling, production of immunoglobulin A is increased⁴³. Thus, our findings presented here are consistent with the hypothesis that $V_{\alpha}19i$ T cells are involved in the homeostasis of gut immunity^{2,7}. We have shown that $V_{\alpha}19i$ T cells help B cells produce



IL-10, which in nonpathogenic conditions may inhibit inflammation against gut flora required for $V_{\alpha}19i$ T cell selection. Therefore, we propose a model of $V_{\alpha}19i$ T cell-induced protection from EAE whereby $V_{\alpha}19i$ T cells interact with B cells in lymphoid tissue through ICOS-B7RP-1 and to a lesser degree through other costimulatory pathways to induce IL-10 production, which in turn can inhibit the production of disease-promoting T_H1 cytokines such as IFN- γ and TNF. In conclusion, here we have identified a protective function for invariant $V_{\alpha}19i$ T cells in autoimmune disease. In contrast to 'conventional' $V_{\alpha}14i$ NKT cells, more T cells express the $V_{\alpha}19i$ TCR human homolog $V_{\alpha}7.2-J_{\alpha}33$ than in mice and therefore these cells may prove to be useful therapeutic targets for the treatment of autoimmune disease.

METHODS

Mice and induction of EAE. C57BL/6 mice (CLEA Laboratory Animal), μ MT mice (Jackson Laboratories), $V_{\alpha}19i$ Tg mice⁵, $V_{\alpha}19i$ Tg $Cd1d1^{-/-}$ mice, $Cd1d1^{-/-}$ mice and $Mrl^{-/-}$ mice⁷ were maintained in specific pathogen-free conditions in accordance with institutional guidelines (National Institute of Neuroscience, Tokyo, Japan.). $Mrl^{-/-}$ mice were backcrossed to C57BL/6 mice for ten generations²⁴. Mice were injected subcutaneously with 100 μ g MOG(35-55) and 1 mg heat-killed *Mycobacterium tuberculosis* H37RA (Difco) emulsified in complete Freund's adjuvant. Pertussis toxin (200 ng in PBS; List Biological Laboratories) was injected intraperitoneally on days 0 and 2 after immunization. EAE clinical symptoms were assigned scores daily as follows: 0, no clinical signs; 1, loss of tail tonicity; 2, impaired righting reflex; 3, partial hindlimb paralysis; 4, total hindlimb paralysis.

Cell sorting and adoptive transfer. For depletion of NK cells, mice were injected intraperitoneally with 100 μ g anti-asialo-GM1 (ref. 44) 48 h before purification of $V_{\alpha}19i$ T cells. Liver or spleen cells were isolated from mice by Percoll density-gradient centrifugation, and NKT cells, B cells and T cells were purified with the AutoMACS cell purification system (Miltenyi Biotech). NKT cells were isolated using phycoerythrin-conjugated anti-NK1.1 (PK136; BD Pharmingen) and anti-phycoerythrin microbeads (Miltenyi Biotech). The purity of isolated NK1.1⁺ T cells, assessed by flow cytometry, was more than 90%. In some experiments, single-cell suspensions were incubated with fluorescein isothiocyanate-anti-CD3 (2C11; BD Pharmingen) and phycoerythrin-anti-NK1.1 (PK136, BD Pharmingen) for sorting by flow cytometry. B cells and T cells were isolated from the spleen with anti-CD19 microbeads or the 'pan T cell' kit (Miltenyi Biotech). For adoptive transfer studies, liver CD3⁺NK1.1⁺ $V_{\alpha}19i$ T cells were sorted from naive $V_{\alpha}19i$ Tg $Cd1d1^{-/-}$ mice as described above, and 1×10^6 $V_{\alpha}19i$ T cells were injected intraperitoneally into naive C57BL/6 recipient mice on the day of immunization with MOG(35-55). Control groups received identical numbers of CD3⁺NK1.1⁻ hepatic cells.

Cell proliferation and cytokine analysis. For *in vitro* stimulation of sorted $V_{\alpha}19i$ T cells, CD3⁺NK1.1⁺ and CD3⁺NK1.1⁻ cells were suspended in RPMI 1640 medium (Sigma) supplemented with 10% FCS, 2 mM L-glutamine, 100 U/ml of penicillin-streptomycin, 2 mM sodium pyruvate and 50 μ M β -mercaptoethanol and were stimulated with immobilized anti-CD3 (5 μ g/ml; BD Pharmingen). Cytokines were measured with inflammation cytometric bead assay kits (BD Biosciences) at 24, 48 and 72 h after stimulation with mouse T_H1 - T_H2 cytokines. At 10 d after EAE induction without pertussis toxin, myelin-specific T cell responses were measured. Lymphocytes (1×10^6) were cultured with MOG(35-55) (1-100 μ M for proliferation studies and 100 μ M for cytokine analysis). Cytokines were measured with a cytometric bead assay kit (BD Biosciences) or an IL-17 enzyme-linked immunosorbent assay kit (BD Pharmingen) at 72 h after stimulation. Identical sets of wells were used for proliferation studies. After 72 h, cells were incubated with [³H]thymidine (1 μ Ci/well) for the final 16 h of culture and incorporation of radioactivity was analyzed with a β -1205 counter (Pharmacia). Proliferation was determined from triplicate wells for each peptide concentration and is expressed as counts per minute.

Surface marker analysis, quantification of CNS leukocytes and histology. The surface phenotype of sorted $V_{\alpha}19i$ T cells was analyzed by flow cytometry. Nonspecific staining was inhibited by incubation with anti-CD16/32 (BD Pharmingen). Cells were then stained with fluorescence-labeled antibodies specific for CD4, NK1.1, TCR β , CD3, CD44, CD49d, CD19, CD8, CD14, CD28, CD278, CD86 or CD154 (BD Pharmingen) or CCR1 and CCR2 (Santa Cruz), followed by phycoerythrin-conjugated anti-goat immunoglobulin G (Santa Cruz), and were analyzed with a FACSCalibur (Becton Dickinson). Intracellular cytokines were analyzed by flow cytometry with the BD Cytotoxic/Cytoperm kit (BD Pharmingen). Staining of paraffin-embedded spinal cords with luxol fast blue and with haematoxylin and eosin was done by SRL. For quantification by flow cytometry, spinal cords were homogenized through 70- μ m nylon mesh and by Percoll density-gradient centrifugation to form single-cell suspensions.

RNA extraction and real-time RT-PCR. The SV Total RNA isolation kit (Promega) was used for isolation of total RNA from sorted liver or splenic NKT cells, T cells or B cells according to the manufacturer's instructions. First-strand cDNA was generated with the Advantage-RT kit (Clontech). The Light Cycler-FastStart DNA Master SYBR Green I kit (Roche Diagnostics) was used for real-time PCR. Gene expression values were normalized to expression of the hypoxanthine guanine phosphoribosyl transferase (*Hprt1*) 'housekeeping' gene. Primers from Bex Co are listed in Supplementary Table 1 online.

Mixed-lymphocyte experiments. MOG(35-55)-specific spleen cells (2×10^6) isolated from wild-type nontransgenic mice 10 d after EAE induction were mixed with liver $V_{\alpha}19i$ T cells (5×10^5) sorted from naive $V_{\alpha}19i$ Tg $Cd1d1^{-/-}$ mice, in the presence of 100 μ g/ml of MOG(35-55) in 24-well plates or transwell plates (Corning). Where indicated, MOG(35-55)-specific spleen cells were isolated from $Mrl^{-/-}$ or μ MT mice or were subjected to depletion with anti-CD19 microbeads (Miltenyi Biotech). Costimulatory molecules were blocked with 10 μ g/ml of anti-B7RP-1 (HK5.3) or anti-CD40L (MR1) or with anti-CD80 and anti-CD86 (16-10A1 and GL1, respectively; all from BD Pharmingen)³⁵. After 72 h, cytokines in the supernatant were analyzed by cytometric bead assay, enzyme-linked immunosorbent assay or intracellular flow cytometry. Proliferation of MOG(35-55)-specific lymph node cells was assessed 24 h after the addition of [³H]thymidine (1 μ Ci/well) to 96-well plates.

Statistics. EAE clinical scores for groups of mice are presented as the mean group clinical score \pm s.e.m., and statistical differences were analyzed by the Mann-Whitney U nonparametric ranking test. Cytokine secretion data were analyzed with the two-tailed Student's *t*-test or one-way analysis of variance with Tukey post-analysis for multiple group analysis.

Note: Supplementary information is available on the Nature Immunology website.

ACKNOWLEDGMENTS

We thank S. Gilfillan (Department of Pathology and Immunology, Washington University School of Medicine, St. Louis, Missouri) for $Mrl^{-/-}$ mice. Supported by the Japan Society for the Promotion of Science (P03581 to J.L.C.), the Ministry of Health, Labour and Welfare of Japan (T.Y. and S.M.), The Program for Promotion of Fundamental Studies in Health Sciences of the National Institute of Biomedical Innovation (02-5 to T.Y.), Grant-in-Aid for Science Research on Priority Area from Ministry of Education, Science, Sports and Culture of Japan (17047051 to S.M.) and Grant-in-Aid for Scientific Research (B) (18390295 to S.M.) from the Japan Society for the Promotion of Science.

COMPETING INTERESTS STATEMENT

The authors declare that they have no competing financial interests.

Published online at <http://www.nature.com/natureimmunology/>
Reprints and permissions information is available online at <http://npg.nature.com/reprintsandpermissions/>

1. Kronenberg, M. Toward an understanding of NKT cell biology: progress and paradox. *Annu. Rev. Immunol.* **23**, 877-900 (2005).
2. Treiner, E. *et al.* Mucosal-associated invariant T (MAIT) cells: an evolutionarily conserved T cell subset. *Microbes Infect.* **7**, 552-559 (2005).
3. Kawano, T. *et al.* CD1d-restricted and TCR-mediated activation of $V_{\alpha}14$ NKT cells by glycosylceramides. *Science* **278**, 1626-1629 (1997).

4. Zhou, D. *et al.* Lysosomal glycosphingolipid recognition by NKT cells. *Science* **306**, 1786–1789 (2004).
5. Okamoto, N. *et al.* Synthetic α -mannosyl ceramide as a potent stimulant for an NKT cell repertoire bearing the invariant V α 19-J α 26 TCR α chain. *Chem. Biol.* **12**, 677–683 (2005).
6. Chen, Y.H., Chiu, N.M., Mandal, M., Wang, N. & Wang, C.R. Impaired NK1⁺ T cell development and early IL-4 production in CD1-deficient mice. *Immunity* **6**, 459–467 (1997).
7. Treiner, E. *et al.* Selection of evolutionarily conserved mucosal-associated invariant T cells by MR1. *Nature* **422**, 164–169 (2003).
8. Spada, F.M., Koezuka, Y. & Porcelli, S.A. CD1d-restricted recognition of synthetic glycolipid antigens by human natural killer T cells. *J. Exp. Med.* **188**, 1529–1534 (1998).
9. Tilloy, F. *et al.* An invariant T cell receptor α chain defines a novel TAP-independent major histocompatibility complex class Ib-restricted $\alpha\beta$ T cell subpopulation in mammals. *J. Exp. Med.* **189**, 1907–1921 (1999).
10. Godfrey, D.I., MacDonald, H.R., Kronenberg, M., Smyth, M.J. & Van Kaer, L. NKT cells: what's in a name? *Nat. Rev. Immunol.* **4**, 231–237 (2004).
11. Lehuen, A. *et al.* Overexpression of natural killer T cells protects V α 14-J α 281 transgenic nonobese diabetic mice against diabetes. *J. Exp. Med.* **188**, 1831–1839 (1998).
12. Mars, L.T. *et al.* V α 14-J α 281 NKT cells naturally regulate experimental autoimmune encephalomyelitis in nonobese diabetic mice. *J. Immunol.* **168**, 6007–6011 (2002).
13. Wagner, M.J., Hussain, S., Mehan, M., Verdi, J.M. & Delovitch, T.L. A defect in lineage fate decision during fetal thymic invariant NKT cell development may regulate susceptibility to type 1 diabetes. *J. Immunol.* **174**, 6764–6771 (2005).
14. Pál, E. *et al.* Costimulation-dependent modulation of experimental autoimmune encephalomyelitis by ligand stimulation of V α 14 NK T cells. *J. Immunol.* **166**, 662–668 (2001).
15. Sharif, S. *et al.* Activation of natural killer T cells by α -galactosylceramide treatment prevents the onset and recurrence of autoimmune type 1 diabetes. *Nat. Med.* **7**, 1057–1062 (2001).
16. Hong, S. *et al.* The natural killer T-cell ligand α -galactosylceramide prevents autoimmune diabetes in non-obese diabetic mice. *Nat. Med.* **7**, 1052–1056 (2001).
17. Miyamoto, K., Miyake, S. & Yamamura, T. A synthetic glycolipid prevents autoimmune encephalomyelitis by inducing T μ 2 bias of natural killer T cells. *Nature* **413**, 531–534 (2001).
18. Chiba, A. *et al.* Suppression of collagen-induced arthritis by natural killer T cell activation with OCH, a sphingosine-truncated analog of α -galactosylceramide. *Arthritis Rheum.* **50**, 305–313 (2004).
19. Miyake, S. & Yamamura, T. Therapeutic potential of glycolipid ligands for natural killer (NK) T cells in the suppression of autoimmune diseases. *Curr. Drug Targets Immune Endocr. Metabol. Disord.* **5**, 315–322 (2005).
20. Chiba, A., Kaieda, S., Oki, S., Yamamura, T. & Miyake, S. The involvement of V α 14 natural killer T cells in the pathogenesis of arthritis in murine models. *Arthritis Rheum.* **52**, 1941–1948 (2005).
21. Kim, H.Y. *et al.* NKT cells promote antibody-induced joint inflammation by suppressing transforming growth factor β 1 production. *J. Exp. Med.* **201**, 41–47 (2005).
22. Porcelli, S., Yockey, C.E., Brenner, M.B. & Balk, S.P. Analysis of T cell antigen receptor (TCR) expression by human peripheral blood CD4⁺ $\alpha\beta$ T cells demonstrates preferential use of several V μ genes and an invariant TCR α chain. *J. Exp. Med.* **178**, 1–16 (1993).
23. Shimamura, M. & Huang, Y.Y. Presence of a novel subset of NKT cells bearing an invariant V α 19.1-J α 26 TCR α chain. *FEBS Lett.* **516**, 97–100 (2002).
24. Kawachi, I., Maldonado, J., Strader, C. & Gilfillan, S. MR1-restricted V α 19i mucosal-associated invariant T cells are innate T cells in the gut lamina propria that provide a rapid and diverse cytokine response. *J. Immunol.* **176**, 1618–1627 (2006).
25. Illés, Z., Shimamura, M., Newcombe, J., Oka, N. & Yamamura, T. Accumulation of V α 7.2-J α 33 invariant T cells in human autoimmune inflammatory lesions in the nervous system. *Int. Immunol.* **16**, 223–230 (2004).
26. Illés, Z. *et al.* Differential expression of NK T cell V α 24J α Q invariant TCR chain in the lesions of multiple sclerosis and chronic inflammatory demyelinating polyneuropathy. *J. Immunol.* **164**, 4375–4381 (2000).
27. Croxford, J.L., Feldmann, M., Chernajovsky, Y. & Baker, D. Different therapeutic outcomes in experimental allergic encephalomyelitis dependent upon the mode of delivery of IL-10: a comparison of the effects of protein, adenoviral or retroviral IL-10 delivery into the central nervous system. *J. Immunol.* **166**, 4124–4130 (2001).
28. Croxford, J.L. *et al.* Cytokine gene therapy in experimental allergic encephalomyelitis by injection of plasmid DNA-cationic liposome complex into the central nervous system. *J. Immunol.* **160**, 5181–5187 (1998).
29. Cua, D.J., Groux, H., Hinton, D.R., Stohman, S.A. & Coffman, R.L. Transgenic interleukin 10 prevents induction of experimental autoimmune encephalomyelitis. *J. Exp. Med.* **189**, 1005–1010 (1999).
30. Bettelli, E., Nicholson, L.B. & Kuchroo, V.K. IL-10, a key effector regulatory cytokine in experimental autoimmune encephalomyelitis. *J. Autoimmun.* **20**, 265–267 (2003).
31. Langrish, C.L. *et al.* IL-23 drives a pathogenic T cell population that induces autoimmune inflammation. *J. Exp. Med.* **201**, 233–240 (2005).
32. Fillatreau, S., Sweeney, C.H., McGeachy, M.J., Gray, D. & Anderton, S.M. B cells regulate autoimmunity by provision of IL-10. *Nat. Immunol.* **3**, 944–950 (2002).
33. Mauri, C., Gray, D., Mushtaq, N. & Londei, M. Prevention of arthritis by interleukin 10-producing B cells. *J. Exp. Med.* **197**, 489–501 (2003).
34. Riegert, P., Wanner, V. & Bahram, S. Genomics, isoforms, expression, and phylogeny of the MHC class I-related MR1 gene. *J. Immunol.* **161**, 4066–4077 (1998).
35. Hayakawa, Y. *et al.* Differential regulation of Th1 and Th2 functions of NKT cells by CD28 and CD40 costimulatory pathways. *J. Immunol.* **166**, 6012–6018 (2001).
36. Ikarashi, Y. *et al.* Dendritic cell maturation overrules H-2D-mediated natural killer T (NKT) cell inhibition: critical role for B7 in CD1d-dependent NKT cell interferon γ production. *J. Exp. Med.* **194**, 1179–1186 (2001).
37. Kitamura, H. *et al.* The natural killer T (NKT) cell ligand α -galactosylceramide demonstrates its immunopotentiating effect by inducing interleukin (IL)-12 production by dendritic cells and IL-12 receptor expression on NKT cells. *J. Exp. Med.* **189**, 1121–1128 (1999).
38. Kaneda, H. *et al.* ICOS costimulates invariant NKT cell activation. *Biochem. Biophys. Res. Commun.* **327**, 201–207 (2005).
39. Hutloff, A. *et al.* ICOS is an inducible T-cell co-stimulator structurally and functionally related to CD28. *Nature* **397**, 263–266 (1999).
40. McAdam, A.J. *et al.* ICOS is critical for CD40-mediated antibody class switching. *Nature* **409**, 102–105 (2001).
41. Song, F. *et al.* Expression of the neutrophil chemokine KC in the colon of mice with enterocolitis and by intestinal epithelial cell lines: effects of flora and proinflammatory cytokines. *J. Immunol.* **162**, 2275–2280 (1999).
42. Kaneko, M., Akiyama, Y., Takimoto, H. & Kumazawa, Y. Mechanism of up-regulation of immunoglobulin A production in the intestine of mice unresponsive to lipopolysaccharide. *Immunology* **116**, 64–70 (2005).
43. Cognasse, F. *et al.* Differential downstream effects of CD40 ligation mediated by membrane or soluble CD40L and agonistic Ab: a study on purified human B cells. *Int. J. Immunopathol. Pharmacol.* **18**, 65–74 (2005).
44. Muhlen, K.A. *et al.* NK cells, but not NKT cells, are involved in *Pseudomonas aeruginosa* exotoxin A-induced hepatotoxicity in mice. *J. Immunol.* **172**, 3034–3041 (2004).

